European Economic Review 186 (2026) 105327

Contents lists available at ScienceDirect

European Economic Review

journal homepage: www.elsevier.com/locate/eer

Extreme weather in Europe: Determinants and economic impact☆,☆☆

Marcelle Chauvet [a,c], Claudio Morana [b,c,d,e,*], Murilo Silva [f]

[a] University of California-Riverside, United States of America
[b] University of Milano-Bicocca, Italy
[c] The Rimini Centre for Economic Analysis (RCEA), United States of America
[d] The Rimini Centre for Economic Analysis - Europe (RCEA-Europe), Italy
[e] Center for European Studies (CefES-DEMS), Italy
[f] Union College, United States of America

ARTICLE INFO

JEL classification:
C21
C23
Q51
Q54

Keywords:
Climate change
Extreme weather events
Global warming
GHG emissions
Economic impact and transmission mechanism of climate change
Trend-cycle decomposition
Dynamic panel model
Europe

ABSTRACT

This paper investigates the relationship between anthropogenic greenhouse gas (GHG) emissions and extreme weather conditions in Europe using a novel panel regression trend–cycle decomposition approach. Using the European Extreme Events Climate Index (E3CI) and its seven subcomponents for 40 European countries since 1981, the study finds a significant statistical association between extreme weather deterioration and both the flow and the stock dimensions of global greenhouse gas emissions. Building on these results, dynamic panel regressions within an Autometrics and model-averaging framework reveal significant contractions in GDP growth determined by worsening climatological conditions. The largest effects are observed in the services sector, and extreme wind and precipitation events are the most damaging. Climate deterioration operates through both supply and demand channels – particularly via private spending and productivity – and contributes to structural economic divergence across Europe. Effective mitigation and sustainable economic development are the most powerful tools to counter these adverse effects, while adaptation and institutional improvements serve as second-best measures, particularly against wildfires and extreme temperatures.

1. Introduction

Greenhouse gas (GHG) concentrations have risen steadily since the Industrial Revolution due to human activities, ultimately driving an increase in the Earth's surface temperature — a phenomenon known as global warming. In this context, Europe represents a particularly relevant case study, as it is warming twice as fast as the global average and may thus serve as an indicator of future climate conditions in other regions under unabated GHG emissions. Average land temperatures in Europe have risen sharply over the past four decades, with the trend accelerating in recent years. Over the last ten (five) years, Europe was 2.19°C (2.4°C) warmer

☆ This article is part of a Special issue entitled: 'Climate III' published in European Economic Review.

☆☆ This paper was presented at the 2025 Climate Finance Conference (Comillas University), the 2025 Econometric Models of Climate Change (EMCC) Conference (Victoria University), the 2025 GRETA C.R.E.D.I.T. Conference (University of Venice), and at seminars at the University of Victoria and the European Central Bank. We thank conference participants, discussants, the editor, and two anonymous reviewers for their constructive and insightful comments. We are also grateful to Germanwatch, the NewClimate Institute, and the Climate Action Network for providing access to the CCPI index.

* Correspondence to: Università di Milano - Bicocca, Dipartimento di Economia, Metodi Quantitativi e Strategie di Impresa, Piazza dell'Ateneo Nuovo 1, 20126, Milano, Italy.
E-mail address: claudio.morana@unimib.it (C. Morana).

https://doi.org/10.1016/j.euroecorev.2026.105327
Received 6 January 2025; Received in revised form 10 March 2026; Accepted 14 March 2026
Available online 30 March 2026

than the pre-industrial baseline and 1.47°C warmer than the 1991–2020 reference period (EEA, 2024a). All ten of the warmest years have occurred since 2000. Projections suggest that temperatures across European land areas will continue to rise throughout the century at a pace exceeding the global average (EEA, 2024c).

As the climate has warmed, the frequency and intensity of extreme weather events have risen worldwide. In the EU alone, weather and climate-related extremes caused an estimated €738 billion in economic losses between 1980 and 2023, with more than €162 billion in the 2021–2023 period alone. Most damage stems from floods (44%), storms (29%), and heatwaves (19%), and is projected to increase further under unabated greenhouse gas emissions and ongoing climate change (EEA, 2024b). The costs of inaction or delayed climate policy are expected to exceed those of proactive mitigation and adaptation, particularly in more vulnerable EU regions (Dellink et al., 2019; Kahn et al., 2021; Szewczyk et al., 2020; Guo et al., 2021; Usman et al., 2025), consistent with evidence from other world regions (Auffhammer, 2018; Bilal and Stock, 2025; Kiley, 2024; Orlov et al., 2020). Early cross-country estimates indicate that an average storm reduces GDP growth on impact by 0.16%, an average drought by 0.01%, and an average extreme-temperature event by 0.05% (Felbermayr and Gröschl, 2014).

The economic consequences of climate change are most pronounced under high-warming, business-as-usual scenarios. Yet, they remain substantial even under stringent mitigation pathways such as the Paris-aligned RCP2.6 (2°C target). Kahn et al. (2021) estimate contractions in GDP per capita of up to 0.8% by 2030, 2.35% by 2050, and 6.69% by 2100 under RCP8.5. Controlling for automation deepening, Orlov et al. (2020) find that heat-induced productivity losses would reduce global GDP by 1.4%–1.8% by 2100 under RCP8.5, while the decline would moderate to around 0.5% under RCP2.6. Although successful adaptation could significantly mitigate these losses, it cannot eliminate them.

Recent research has further clarified the mechanisms driving the persistent GDP contractions projected by climate models (Szewczyk et al., 2020; Dellink et al., 2019). A growing body of evidence shows that the economic effects of extreme weather events are long-lasting, affecting both current and potential output (Parker, 2023). Bodenstein and Scaramucci (2025) estimate that severe disasters lead to persistent GDP losses, with output falling by roughly 2% over the medium term (5–7 years) and failing to recover fully after a decade. Usman et al. (2025) document similarly adverse medium-term effects across EU countries. These events damage physical capital and infrastructure, reduce usable land, and impair production efficiency through heat stress, supply-chain disruptions, and technological regressions.

García-León et al. (2021) find that heatwaves in 2003, 2010, 2015, and 2018 caused total European GDP losses of 0.3%–0.5%, with peaks exceeding 1% in more vulnerable regions. Kimmich et al. (2025) provide further evidence on heatwave transmission mechanisms, estimating sector-specific labor-productivity losses ranging from 0.2% to 3%, with agriculture and construction being the most exposed. Caggese et al. (2025) identify a highly nonlinear relationship between temperature and productivity, estimating aggregate productivity declines of 1.7% and 6.8% in response to 2°C and 4°C increases in average annual temperature, respectively — effects that are likely to be particularly severe in Southern Europe.

Prolonged heatwaves and a shifting climate also induce inefficient adaptation investments (Noy and Strobl, 2023; Bijnens et al., 2024; Dietz and Lanz, 2025) and further disrupt labor supply through heat stress and climate-related migration (Bier, 2017). Kotz et al. (2022) highlight the damaging effects of extreme rainfall, especially in high-income countries, while sea-level rise and river/coastal flooding pose significant risks to Northern and Central Europe. Cortés Arbués et al. (2024) estimate GDP losses of around 1.3% for the EU plus the UK due to climate-driven sea-level rise. However, impacts are highly heterogeneous, with some coastal regions facing losses of 10%–20%.

On the demand side, rising uncertainty, income losses, precautionary savings, and displacement weaken consumption and investment, amplifying supply-side disruptions (Natoli, 2023; Usman et al., 2025). Gagliardi et al. (2022) warn that extreme weather events may also threaten fiscal sustainability in several EU countries. Overall, climate change presents a complex and uneven economic landscape for Europe, with the potential to exacerbate income divergence across individuals, sectors, and regions (Breckenfelder et al., 2023).

In light of the above evidence, this paper further examines the economic implications of deteriorating extreme weather conditions in Europe, providing original methodological and empirical contributions to the existing literature. Methodologically, we build on Morana (2024) and Morana and Sbrana (2019) and introduce a novel multivariate trend-cycle decomposition within a panel regression setting. This approach is used to examine how anthropogenic GHG emissions drive underlying extreme weather patterns. It is particularly well-suited to this task, as it exploits cross-country and temporal variation in extreme weather events, conditioning the extraction of the trend component on their likely common determinant – GHG emissions – while controlling for nonlinearities and cross-country heterogeneity. It also indirectly accounts for natural phenomena that may influence low-frequency weather behavior. The framework is grounded in the notion that climate change is a global externality: emissions from one country contribute to the worldwide stock of heat-trapping gases, thereby increasing the severity and frequency of extreme events worldwide.

Our analysis covers 40 European countries over the period 1981–2023. It is based on the European Extreme Events Climate Index (E3CI) and its seven subcomponents: extreme maximum and minimum temperatures, wind speed, precipitation, droughts, wildfires, and hail. To our knowledge, this dataset has not previously been analyzed in the literature. We find that the common component of extreme weather behavior – associated with anthropogenic GHG emissions and potentially natural forces – is dominant over idiosyncratic components, consistent with the global nature of climate change and the additional influence of long-period natural oscillators. This result aligns with recent findings by Bilal and Kanzig (2024), who emphasize the importance of accounting for common effects in climate change research.

Second, we estimate the GDP costs of climate change under a business-as-usual scenario, examining its sectoral composition and the supply- and demand-side transmission mechanisms. We also assess the role of adaptation and mitigation policies, as well as institutional and economic development, in moderating these costs, while controlling for geographical factors. Our analysis

employs a dynamic panel framework, conditioning on the estimated extreme weather trend components derived in the first stage. By controlling for short-term climatic variability and linking trend components to anthropogenic GHG emissions, our approach yields a more accurate assessment of GDP impacts than standard methods using raw data. As an additional methodological refinement, we implement fixed unit and time effects within Autometrics – the automated general-to-specific procedure (Hendry et al., 2008) – to retain only statistically significant controls, thereby improving estimation efficiency and reliability. The use of model averaging techniques further enhances the robustness of our findings and policy implications.

Our findings are broadly consistent with the existing literature on Europe. Yet they also extend it by providing new complementary evidence, offering broader geographic coverage (beyond the EU), a more comprehensive treatment of extreme weather typologies, a longer time horizon, and an in-depth analysis of the demand- and supply-side transmission mechanisms, using new econometric tools.

We show that deteriorating extreme weather conditions significantly contract GDP growth, affecting all its sectoral components, with a most substantial impact on services. Productivity and private spending emerge as the most critical transmission channels on the supply and demand sides, respectively. Extreme precipitation, wind, and wildfires exert the strongest adverse effects on productivity growth. Aggregate consumption is similarly most affected by extreme wind and precipitation. The impact of extreme temperatures on labor productivity and aggregate consumption is nonlinear, with negative effects for maximum temperatures and positive effects for minimum temperatures. Private investment is predominantly negatively affected by rising extreme temperatures, both minimum and maximum.

Moreover, labor productivity is most affected in Southern and relatively warmer countries, while total factor productivity is primarily impacted in Northern and relatively cooler regions. Efficiency losses are more pronounced in Eastern Europe compared to Western Europe. These losses are generally larger in countries with weaker adaptation and mitigation policies, fragile institutions, and lower income levels. The impact on aggregate consumption and investment is also more substantial in countries with weaker mitigation frameworks. Interestingly, the adverse effects on private spending responses appear more significant in Northern, Western, and cooler European countries, as well as in those with stronger institutions and adaptation policies. Hence, climate change is not only a macroeconomic disruptor but also a catalyst for structural divergence across Europe.

From a policy perspective, mitigation strategies and sustainable economic development appear to be the most effective tools for reducing the contribution of worsening extreme weather conditions to economic stagnation and structural divergence — particularly those stemming from extreme precipitation and wind. Adaptation policies and institutional development, while valuable, are second-best instruments, offering relatively stronger protection against wildfires and rising extreme temperatures.

The remainder of the paper is structured as follows. Section 2 presents evidence on extreme weather in Europe. Section 3 introduces a new econometric tool to assess the anthropogenic origin of evolving extreme weather patterns and provides related empirical evidence. Section 4 outlines the econometric strategy used to evaluate the economic impact of climate change, its transmission mechanisms, its divergence effects, and the resulting policy implications. Sections Section 5, 6, and 7 present the corresponding empirical results, and Section 8 concludes. The Online Appendix provides details on the data, model specification, and additional empirical results.

2. Evolving extreme weather in Europe

Our analysis begins with some descriptive evidence on the evolution of extreme weather in Europe. The data investigated covers forty European countries from 1981 to 2023, i.e., Albania, Andorra, Austria, Belarus, Belgium, Bosnia-Herzegovina, Bulgaria, Croatia, Cyprus, Czechia, Denmark, Estonia, Finland, France, Germany, Greece, Hungary, Iceland, Ireland, Italy, Latvia, Lithuania, Luxembourg, Malta, Moldova, Montenegro, the Netherlands, North Macedonia, Norway, Poland, Portugal, Romania, Serbia, Slovakia, Slovenia, Spain, Sweden, Switzerland, Ukraine, and the United Kingdom.

We utilize the European Extreme Events Climate Index (E3CI) and its subcomponents, which provide information on the intensity of extreme maximum and minimum temperatures, precipitation, wind speed, hail, drought, and wildfires. The E3CI index effectively monitors the development of extreme weather realizations over time, yielding an assessment relative to a historical benchmark spanning the 1980–2010 period. Refer to the Online Appendix for data details.

Fig. 1 presents the average annual figures for the last four decades and the most recent 2020–2023 period for the E3CI index and its subcomponents. The aggregate statistics are computed as cross-sectional averages over the forty European countries in the sample. We calculate annual figures by averaging the monthly observations to highlight trend-level changes. We then rescale these statistics so that values larger than one correspond to abnormal realizations for the E3CI index and its subcomponents, i.e., to weather conditions more extreme than in the past (1980 to 2010 average).

As shown in Fig. 1, the E3CI index indicates an increase in extreme weather events over the last fifteen years, which also intensifies over time. The increase in the index on average since 2020 is even more significant than in the previous decade (2010–2019). The evidence suggests that worsening weather conditions and extreme events are becoming more frequent at the trend level.

From Fig. 1, the worsening in average weather conditions, as detected by the E3CI index, can be attributed to its sources. Extreme-heat developments (Max Temp) appear to be the most critical driver of the worsening registered by the E3CI index. Extreme heat conditions have worsened over the last thirty years, with a notable increase in frequency. Specifically, there was a 25% increase in the 2000s compared to the 1990s, followed by a 60% increase in the 2010s over the 2000s, and a further 20% increase in the last four years of the sample compared to the previous decade. By comparing current values with those of the 1980s, the increase in extreme heat frequency is over 180%.

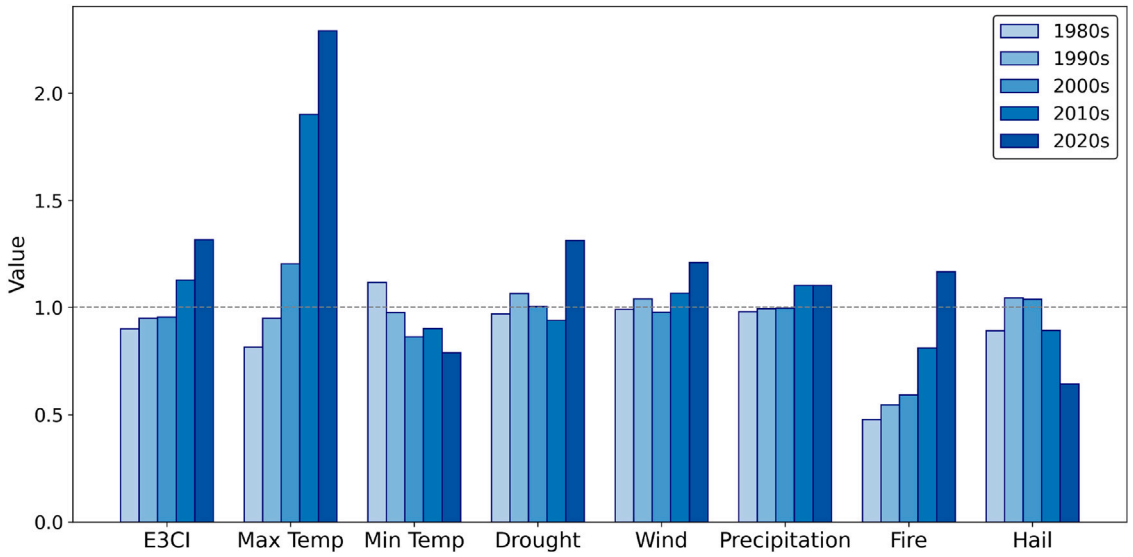

Fig. 1. Extreme weather events in Europe.
Note: This Figure reports average annual values over the last four decades and the most recent 2020–2023 period for the E3CI index and its subcomponents. The aggregate values are computed as cross-sectional averages over the forty European countries in the sample. The values reported are rescaled such that values larger than one are considered abnormal realizations for the E3CI index and its subcomponents, i.e., to weather conditions more extreme than in the past.

Global warming is a two-sided phenomenon. On one side, it leads to hotter summers. On the other hand, it leads to milder winters. The relevance of these implications is evident from Fig. 1, which also reports trend developments in extreme-cold realizations (Min Temp). The overall decrease in the indicator in the most recent period, compared to the 1980s average value, is approximately 30%. The evidence from previous decades shows that these developments have progressed over time. Therefore, the global warming effect appears asymmetric, leading to more frequent extreme heat episodes than less frequent extreme cold episodes.

Wildfires and drought are also phenomena showing an increasing intensity. This finding is consistent with the development of extreme heat. The frequency of drought episodes has increased by 30% in the most recent sample compared to the values in the 1980s. Developments in previous decades were less clear-cut. On the other hand, the frequency of wildfire episodes has been progressive over time. The wildfire indicator shows a 150% increase in frequency in the most recent period compared to the 1980s. While the origin of wildfires is often human-made, their damage depends on their propagation, which in turn depends on weather conditions, particularly air humidity and temperature. In this respect, the global warming effect appears to foster the joint realization of extreme weather events of different types: the frequency increase in drought, wildfire, and heatwave episodes seems to be connected, and the E3CI index fully reflects this connection.

The frequency of extreme precipitation and wind episodes has also increased over the past fifteen years, about 10%–20% relative to the 1980s. The increase in extreme wind frequency is more pronounced in the most recent period (20%) than in the previous decade (10%). On the other hand, the frequency of hail episodes has been decreasing over the last fifteen years. This finding, however, has no implications for the intensity of hailstorms when they occur. In 2023 and 2024, the size of hailstones has been, on average, bigger than in the past (ESWD, 2023). In Northern Italy, the probability of hailstones over five centimeters in diameter is currently 300% higher than it was in the 1980s. In the summer of 2024, a hailstone with a diameter of 19 cm was recorded.

2.1. Assessing trend behavior in extreme weather series

Fig. 2 reports the time series for the aggregate European E3CI index and its seven subcomponents. For graphical purposes, we remove the outlying values for the hail data in 1985 and 2022 and replace them with estimated trend values generated by a structural time series interpolation model.

We formally test for evolving extreme weather conditions by means of the Becker et al. (2006) augmented KPSS test. In particular, we compare results for testing the null hypothesis of level stationarity with the findings obtained for testing the null hypothesis of nonlinear trend stationarity. Considering the generic extreme weather time series $\{y_t\}$, the auxiliary model used for testing is

$$y_t = f(t) + \mu_t + \varepsilon_t \tag{1}$$

where $f(t)$ is the purely deterministic component, $\mu_t = \mu_{t-1} + v_t$, $v_t \sim w.n.(0, \sigma_v^2)$, ε_t is an I(0) process potentially heteroskedastic. Under the null hypothesis, $\sigma_v^2 = 0$ and $\mu_t = \mu_0$, yielding level stationarity if

$$f(t) = \theta_0, \tag{2}$$

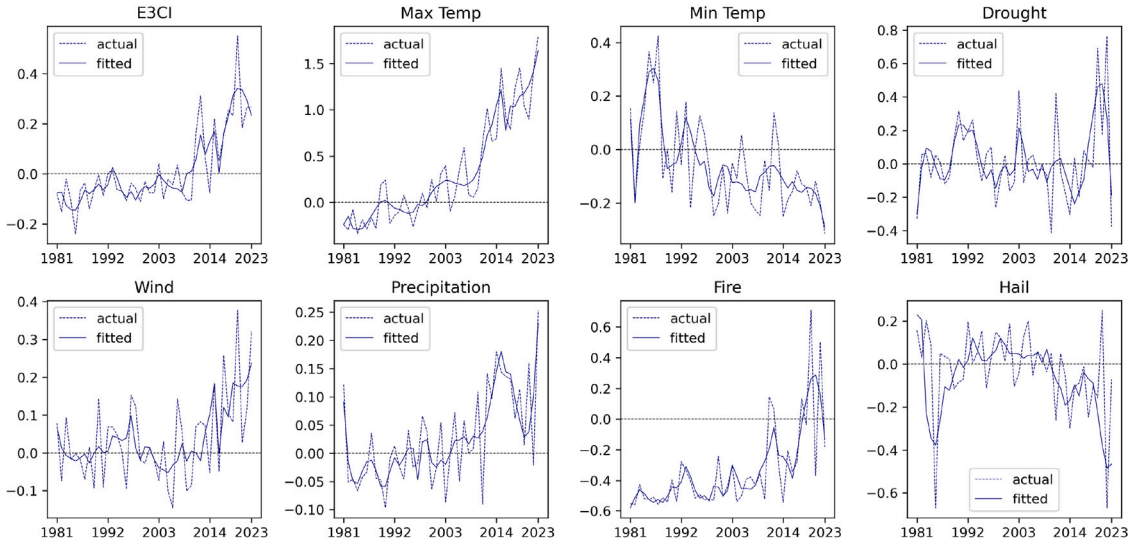

Fig. 2. Evolving extreme weather conditions in Europe.
Note: The figure reports the time series of the actual values and their fitted trend components for the aggregate European E3CI index and its seven subcomponents over the period 1981–2023. The aggregate values are computed as cross-sectional averages over the 40 European countries in the sample.

where θ_0 is a constant term; linear trend stationarity if

$$f(t) = \theta_0 + \theta_1 t, \tag{3}$$

where θ_1 is a parameter and $t = 1, 2, \ldots, T$ the linear time trend; non-linear trend stationarity of order j^* if

$$f(t) = \theta_0 + \sum_{j=1}^{j^*} \theta_{s,j} \sin(2\pi j \frac{t}{T}) + \sum_{j=1}^{j^*} \theta_{c,j} \cos(2\pi j \frac{t}{T}), \tag{4}$$

where $\theta_{s,j}$ and $\theta_{c,j}$ are parameters. The Flexible Fourier form in (4) allows for effective modeling of unknown forms of trend developments, accounting for nonlinear and non-monotonous paths over time, as evident from the descriptive trend analysis. The assumption of a deterministic trend aligns with the statistical properties of the principal driver of evolving extreme weather conditions, namely, the radiative forcing effects of long-lived greenhouse gases such as carbon dioxide (CO_2), methane (CH_4), nitrous oxide (N_2O), and various industrial compounds like chlorofluorocarbons (CFCs). Radiative forcing quantifies the extent to which GHGs disrupt Earth's energy balance, thereby pushing the climate system toward warming (or cooling). It is inherently shaped by policy and technological developments and, as illustrated in Fig. 3, its trajectory is more accurately captured by a segmented trend than by a random walk.

The segmented trend assumption is also consistent with Philippon (2022), who shows that productivity growth follows a piecewise linear (additive) trajectory, shaped by historical regimes and technological transitions. Such a segmented, regime-based view of economic dynamics closely parallels the evolution of radiative forcing. Radiative forcing has progressed through distinct phases, including the coal era, the oil era, and the current decarbonization era, and is responsive to policy interventions and technological shifts. Like productivity growth, its trend reflects structural breaks rather than stochastic drift, reinforcing the appropriateness of a segmented deterministic specification. For example, the reduction in the slope of the NOAA Annual Greenhouse Gas Index (AGGI), our radiative forcing measure, during the 1990s largely reflects the phase-out of specific CFCs initiated in the late 1980s under the Montreal Protocol and the slowdown in the growth rate of atmospheric CO_2, which parallels the productivity slowdown experienced by most OECD countries in the same period (Estrada et al., 2013b; Philippon, 2022). Overall, the radiative forcing time series exhibits clear episodes of acceleration and deceleration, rather than stochastic drift. Formal statistical evidence that radiative forcing variables, like temperature series, are trend stationary processes with time-ordered breaks in the slope of their trend function was initially provided by Estrada et al. (2013a,b), as well as evidence that global temperature series share a common nonlinear trend that is imparted mainly by GHGs' radiative forcing (see also Kaufmann et al., 2006, 2013).

Table 1 and Fig. 4 report the results of the Becker et al. (2006) augmented KPSS tests to provide statistical support for the evolving trends noted in the previous descriptive statistics analysis. In particular, we compare results from testing the null hypothesis of level stationarity with those from testing the null hypotheses of linear and nonlinear trend stationarity. The tests are carried out indicator by indicator on the aggregated annual series obtained from averaging across countries' individual series (Table 1). We also perform the analysis country by country and indicator by indicator. The box-plots in Fig. 4 provide full details of the cross-country distribution of the test statistics applied to the individual series.

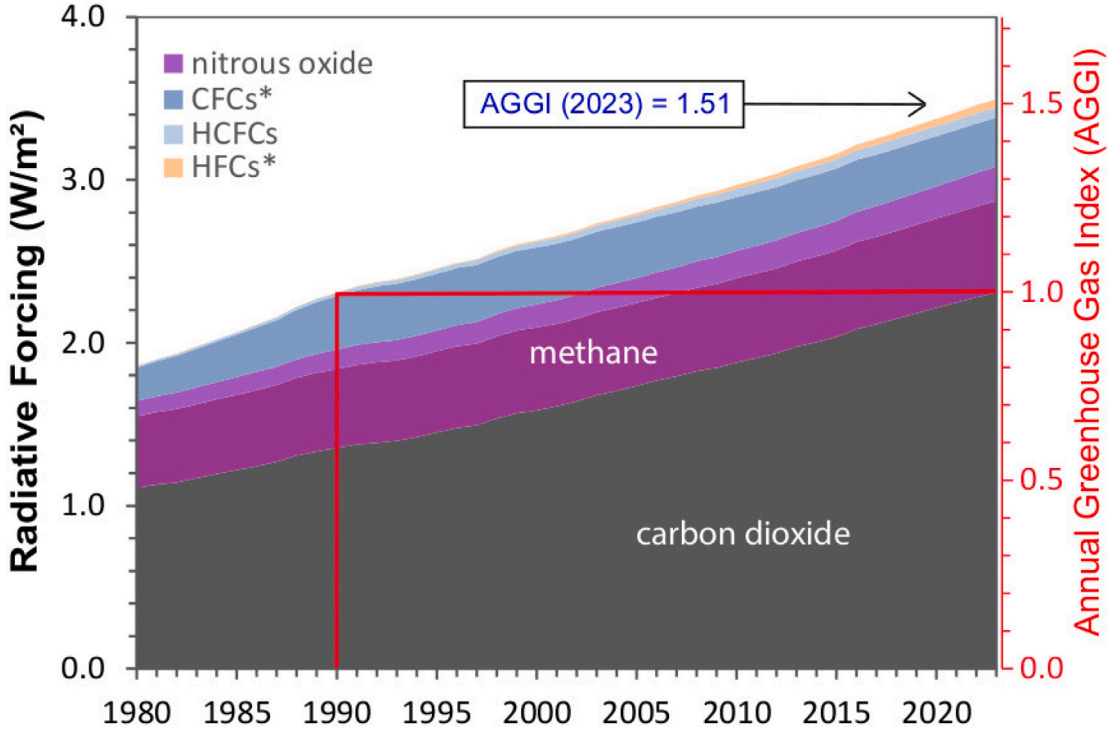

Fig. 3. Radiative forcing and AGGI.
Note: The figure shows the radiative forcing relative to 1750 for virtually all long-lived greenhouse gases. The NOAA Annual Greenhouse Gas Index (AGGI), indexed to 1 in 1990, is displayed on the right-hand axis.
Source: National Oceanic and Atmospheric Administration (NOAA).

Table 1
Stationarity tests for the extreme weather indicators for Europe (aggregates).

	Level	Linear trend	First-order nonlinear trend	Second-order nonlinear trend	Third-order nonlinear trend
E3CI	0.866	0.210	0.091	0.035	0.035
Max Temp	1.063	0.257	0.099	0.042	0.043
Min Temp	0.733	0.073	0.049	0.024	0.083
Drought	0.101	0.087	0.072	0.040	0.037
Wind	0.659	0.202	0.104	0.050	0.045
Precipitation	0.844	0.136	0.043	0.044	0.035
Fire	0.804	0.158	0.065	0.032	0.032
Hail	0.271	0.162	0.047	0.044	0.043
AGGI	0.830	0.107	0.106	0.050	0.035
C.V. 1%	0.739	0.216	0.267	0.162	0.115
C.V. 5%	0.463	0.146	0.169	0.102	0.073

This Table reports the results of the stationarity tests by Becker et al. (2006) for the aggregate values of the E3CI index and its subcomponents, and for the AGGI index. The aggregate values are computed as cross-sectional averages over the forty European countries in the sample. C.V. denotes the critical values at the 1% and 5% significance levels.

As shown in Table 1, the null of level stationarity (column 1) is rejected at the 5% level for the AGGI index, the E3CI index, and all its subcomponents, except for droughts and hail. The rejection is at the 1% level for the AGGI, E3CI, extreme maximum temperature, precipitation, and wildfire components as well. The null of linear trend stationarity (column 2) is also rejected at the 5% level for the E3CI index and its subcomponents, but not for the extreme minimum temperature, drought, and precipitation indicators. Rejection at the 1% level is detected for the extreme maximum temperature. These results suggest that, in general, neither level nor linear trend stationarity well characterizes the dynamic properties of the extreme weather series, possibly pointing to more complex forms of non-stationary behavior, in alternative to stochastic non-stationarity. The results reported in Table 1 (columns 3–5) support this view, as the null hypothesis of nonlinear trend stationarity is never rejected even at the 5% level. The results of the stationarity test carried out on the country-level individual data reported in Fig. 4 further corroborate these findings, showing widespread rejection of the null hypothesis of level stationarity for most indicators and of the null hypothesis of linear trend stationarity, too, albeit to a lesser extent. Yet, the evidence of nonlinear trend stationarity is never rejected for any country or indicator. On the other hand,

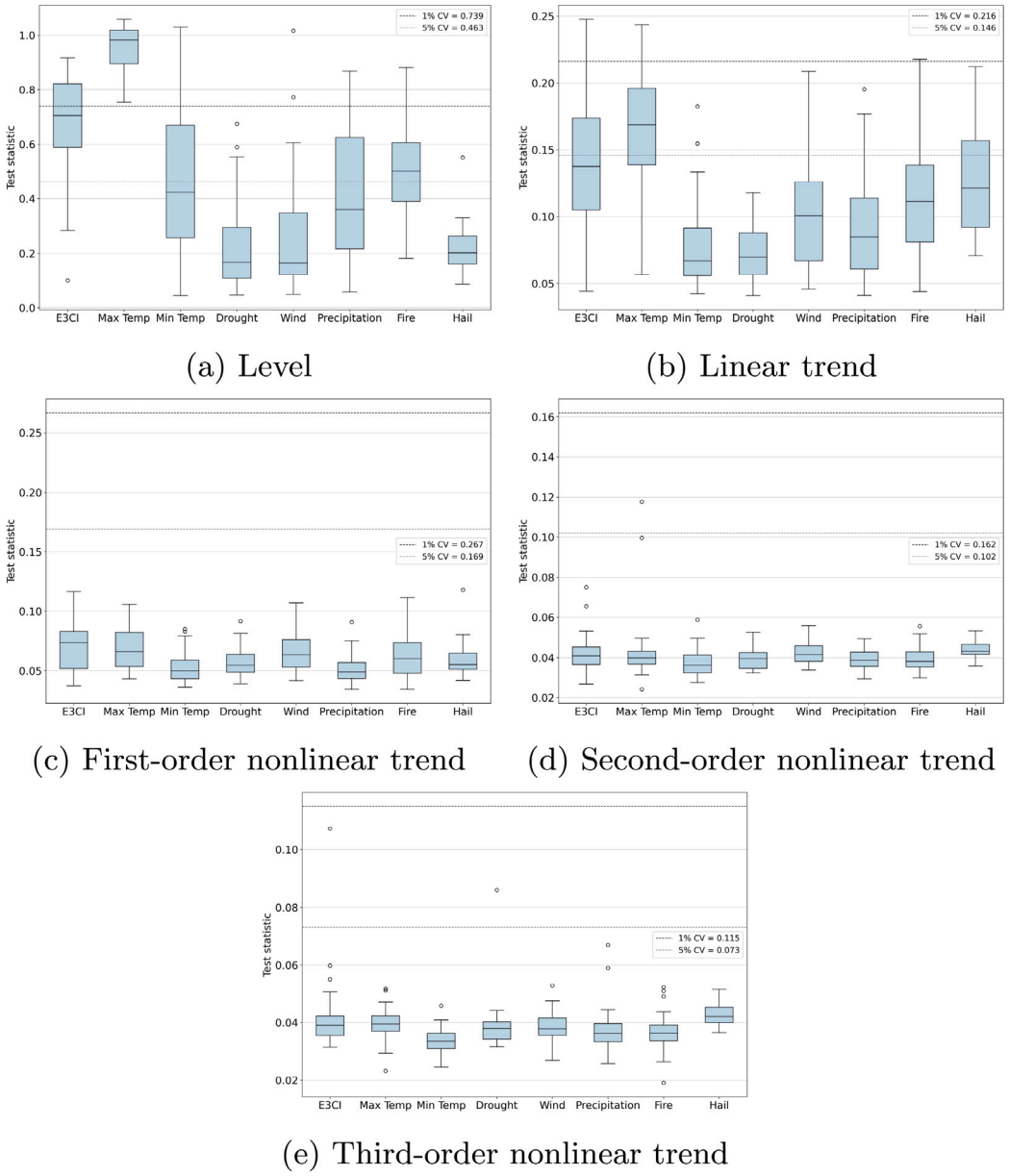

Fig. 4. Stationarity tests for the extreme weather indicators across countries.
Note: This Figure reports the results of the Becker et al. (2006) stationarity tests carried out on the country-level E3CI index and its seven subcomponents for the period 1981–2023.

for the AGGI index, the null hypothesis of trend stationarity is not rejected, and similarly, for the null hypothesis of nonlinear trend stationarity, independent of its parameterization. However, the test statistic decreases as higher degrees of nonlinearity are allowed, consistent with a better fit of the trend function to the series' segmented profile.

Hence, significant nonlinear trends characterize extreme weather events in Europe. Our preferred third-order specification ($j^* = 3$) allows the trend component to describe fluctuations with periodicity larger than 14 years ($P^* = \lfloor T/j^* \rfloor = 14.3$, where $T = 43$). This threshold is motivated by climatological arguments concerning the potential drivers of the trend in these series, i.e., anthropogenic GHG emissions and multidecadal oscillators with long periodicity, such as the Atlantic Multidecadal Oscillation (AMO; 60 to 90 years), avoiding contamination from natural phenomena with shorter periodicity, such as the El Niño-Southern Oscillation (ENSO; 2 to 7 years) and the North Atlantic Oscillation (NAO; 8 to 10 years), and from solar activity (about 11 years). Formal testing of the drivers of evolving extreme weather conditions, specifically about the contribution of human-made GHG emissions, is the object of the following Section. We present a preview of the estimated trend component, delivered by our

comprehensive modeling of underlying extreme weather, in Fig. 2 for the E3CI index and its components. The estimated trends highlight the nonlinearity in their temporal evolution, the origin of which we explore in the following Section.

3. Anthropogenic versus natural drivers of evolving extreme weather

We model underlying extreme weather behavior focusing on each E3CI component at the time. Rather than proceeding sequentially country-by-country, we cast the trend-cycle decomposition approach proposed in Morana (2024) in a panel regression setting, powered by Autometrics (Hendry et al., 2008). This allow the exploitation of likely commonalities of evolving climatic conditions across European countries, increasing efficiency, meanwhile controlling for idiosyncratic short-term variations. For instance, Cassola et al. (2025) find that the E3CI across European countries is well described by four principal components, accounting for about 85% of the total variance. The first PC explains over 50% of the total variance and yields a common European factor. The other PCs carry information on latitude and longitude factors.

Consider the generic n,t element in the vector $\mathbf{y}$, i.e., $y_{n,t}$, $n = 1,\dots,N$, $t = 1,\dots,T$, yielding the tth period observation for the extreme weather indicator $\mathbf{y}$ for the generic nth country. Coherent with data properties, we assume $y_{n,t}$ to be nonlinear-trend stationary. It follows the panel regression

$$
\begin{aligned}
y_{n,t} = & \underbrace{\theta_0 + \sum_{j=0.5}^{j^*} \theta_{s,j} \sin(2\pi j \frac{t}{T}) + \sum_{j=0.5}^{j^*} \theta_{c,j} \cos(2\pi j \frac{t}{T}) +}_{NON-ANTHROPOGENIC\ COMMON\ PART} \\
& \underbrace{\sum_{j=0.5}^{j^*} \theta_{sx,j} \sin(2\pi j x_t^*) + \sum_{j=0.5}^{j^*} \theta_{cx,j} \cos(2\pi j x_t^*) +}_{ANTHROPOGENIC\ COMMON\ PART} \\
& \underbrace{\sum_{n=1}^{N-1} \theta_{0,n} D_{n,t} + \sum_{n=1}^{N-1} \sum_{j=0.5}^{j^*} \theta_{s,n,j} \sin(2\pi j \frac{t}{T}) D_{n,t} + \sum_{n=1}^{N-1} \sum_{j=0.5}^{j^*} \theta_{c,n,j} \cos(2\pi j \frac{t}{T}) D_{n,t} +}_{NON-ANTHROPOGENIC\ IDIOSYNCRATIC\ PART} \\
& \underbrace{\sum_{n=1}^{N-1} \sum_{j=0.5}^{j^*} \theta_{sx,n,j} \sin(2\pi j x_t^*) D_{n,t} + \sum_{n=1}^{N-1} \sum_{j=0.5}^{j^*} \theta_{cx,n,j} \cos(2\pi j x_t^*) D_{n,t} + \varepsilon_{n,t},}_{ANTHROPOGENIC\ IDIOSYNCRATIC\ PART}
\end{aligned} \tag{5}
$$

where $D_{n,t}$ is a dummy variable taking unitary values for country n and zero elsewhere, $t = 1,\dots,T$ is the linear time trend, x_t^* is the AGGI index re-scaled in the interval $[0,1]$, i.e., $x_t^* = (x_t - min(x))/(max(x) - min(x))$, θ_0, $\theta_{s,j}$, $\theta_{c,j}$, $\theta_{sx,j}$, $\theta_{cx,j}$, $\theta_{0,n}$, $\theta_{s,n,j}$, $\theta_{c,n,j}$, $\theta_{sx,n,j}$, $\theta_{cx,n,j}$ are parameters, $\varepsilon_{n,t}$ is a stationary disturbance.

The unknown trend function is approximated by the trigonometric polynomial specification for the conditional mean function in (5). The first five terms in the regression function, whose marginal effects are measured by the parameters θ_0, $\theta_{s,j}$, $\theta_{c,j}$, $\theta_{sx,j}$, $\theta_{cx,j}$ yield the common drivers of evolving *trend* extreme weather conditions across countries; the following five terms, with parameters $\theta_{0,n}$, $\theta_{s,n,j}$, $\theta_{c,n,j}$, $\theta_{sx,n,j}$, $\theta_{cx,n,j}$, capture trend-level heterogeneities across countries. Within each category, we further distinguish the part of non-anthropogenic origin, whose marginal effects are captured by the parameters θ_0, $\theta_{s,j}$, $\theta_{c,j}$, $\theta_{0,n}$, $\theta_{s,n,j}$, $\theta_{c,n,j}$, from the part of anthropogenic origin, with parameters $\theta_{sx,j}$, $\theta_{cx,j}$, $\theta_{sx,n,j}$, $\theta_{cx,n,j}$.

Setting $N = 1$ yields the general trend-cycle model proposed in Morana (2024)

$$
\begin{aligned}
y_{n,t} = & \theta_0 + \sum_{j=0.5}^{j^*} \theta_{s,j} \sin(2\pi j \frac{t}{T}) + \sum_{j=0.5}^{j^*} \theta_{c,j} \cos(2\pi j \frac{t}{T}) + \\
& \sum_{j=0.5}^{j^*} \theta_{sx,j} \sin(2\pi j x_t^*) + \sum_{j=0.5}^{j^*} \theta_{cx,j} \cos(2\pi j x_t^*) + \varepsilon_{n,t}.
\end{aligned} \tag{6}
$$

The model in (6) generalizes (Muller and Watson, 2018), as it allows the extraction of the trend component in the extreme weather indicators by conditioning on information available on its potential driver, i.e., GHGs' radiative forcing (the AGGI index x_t^*). In fact, by setting $\theta_{sx,j} = \theta_{cx,j} = \theta_{sx,n,j} = \theta_{cx,n,j} = 0$, $j = 0.5, 1, 2, \dots, j^*$, and noting that $\sin(z) = \cos(z - \pi/2)$, for $z \in [0,1]$, the model can be rewritten as a function of cosine terms only, delivering the trend components of the series of interest as its cosine transform up to order j^*, as in Muller and Watson (2018). On the other hand, conditioning on the Fourier transforms of the AGGI index, too, as in Morana (2024) and in our further extension, makes the modeling of the underlying developments in extreme weather more comprehensive and, potentially, more accurate. Conditioning on the transformed AGGI – effectively applying a time-deformation – makes the extraction of the underlying trend explicitly dependent on the time-varying pace of greenhouse gas accumulation. Under a standard linear time scale, this variation would be only crudely approximated, since a constant-pace progression cannot capture shifts in the speed at which radiative forcing has increased over time (see also Stock, 1988; Morana and Sbrana, 2019; Robinson, 2021). In their context, Muller and Watson (2018) establish consistency and asymptotic normality of the OLS estimator also under I(1) non-stationarity, thereby ensuring the validity of the trend estimation procedure beyond the trend-stationary case discussed in Morana (2024). Refer to Morana (2024) for Monte Carlo evidence as well.

3.1. Specification issues

Due to the AGGI index's segmented trend behavior, the separation of the anthropogenic and natural contributions foreseen under the model in (5) is unlikely to be feasible in our application, due to the potentially high (positive) correlation between selected pairs of regressors, such as $\sin(2\pi j\frac{t}{T})$ and $\sin(2\pi j x_t^*)$ or $\cos(2\pi j\frac{t}{T})$ and $\cos(2\pi j x_t^*)$, $j = 1, \dots, 3$. Yet, this issue affects only the common parts of the model, because the idiosyncratic parts are nearly orthogonal to both themselves and the common components. Therefore, while the marginal idiosyncratic effects measured by $\theta_{sx,n,j}$, $\theta_{cx,n,j}$, $\theta_{s,n,j}$, $\theta_{c,n,j}$ can be identified, the common marginal effects measured by $\theta_{sx,j}$, $\theta_{cx,j}$, $\theta_{s,j}$, $\theta_{c,j}$ are unlikely to be identified.

To better highlight this issue, the model can be rewritten in its equivalent blockwise rotated form, yielding

$$y_{n,t} = \underbrace{\sum_{j=0.5}^{j^*} \frac{\theta_{sx,j} - \theta_{s,j}}{2} sd_{jt} + \sum_{j=0.5}^{j^*} \frac{\theta_{cx,j} - \theta_{c,j}}{2} cd_{jt}}_{DIFFERENCE\ COMMON\ PART} + \underbrace{\sum_{j=0.5}^{j^*} \frac{\theta_{sx,j} + \theta_{s,j}}{2} sl_{jt} + \sum_{j=0.5}^{j^*} \frac{\theta_{cx,j} + \theta_{c,j}}{2} cl_{jt}}_{LEVEL\ COMMON\ PART} +$$
$$\underbrace{\sum_{n=1}^{N-1} \sum_{j=0.5}^{j^*} \frac{\theta_{sx,n,j} - \theta_{s,n,j}}{2} sd_{jt} D_{n,t} + \frac{\theta_{cx,n,j} - \theta_{c,n,j}}{2} cd_{jt} D_{n,t}}_{DIFFERENCE\ IDIOSYNCRATIC\ PART} +$$
$$\underbrace{\sum_{n=1}^{N-1} \sum_{j=0.5}^{j^*} \frac{\theta_{sx,n,j} + \theta_{s,n,j}}{2} sl_{jt} D_{n,t} + \frac{\theta_{cx,n,j} + \theta_{c,n,j}}{2} cl_{jt} D_{n,t}}_{LEVEL\ IDIOSYNCRATIC\ PART} +$$
$$\underbrace{\theta_0 + \sum_{n=1}^{N-1} \theta_{0,n} D_{n,t}}_{LEVEL\ FIXED\ IIOSYNCRATIC\ PART} + \varepsilon_{n,t}, \tag{7}$$

where the rotated regressors are defined as

$$sd_{j,t} = \sin(2\pi j x_t^*) - \sin(2\pi j\frac{t}{T}), \tag{8}$$

$$cd_{j,t} = \cos(2\pi j x_t^*) - \cos(2\pi j\frac{t}{T}), \tag{9}$$

$$sl_{j,t} = \sin(2\pi j x_t^*) + \sin(2\pi j\frac{t}{T}), \tag{10}$$

$$cl_{j,t} = \cos(2\pi j x_t^*) + \cos(2\pi j\frac{t}{T}). \tag{11}$$

Then, without lack of generality, consider the simplified model where only the common components are retained (the near orthogonal idiosyncratic terms are dropped), and all the variables are zero mean (the constant is dropped too)

$$y_{n,t} = \underbrace{\sum_{j=0.5}^{j^*} \beta_{sd,j} sd_{jt} + \sum_{j=0.5}^{j^*} \beta_{cd,j} cd_{jt}}_{DIFFERENCE\ COMMON\ PART} + \underbrace{\sum_{j=0.5}^{j^*} \beta_{sl,j} sl_{jt} + \sum_{j=0.5}^{j^*} \beta_{cl,j} cl_{jt}}_{LEVEL\ COMMON\ PART} + \varepsilon_{n,t}, \tag{12}$$

where $\beta_{sd,j} = \frac{\theta_{sx,j} - \theta_{s,j}}{2}$, $\beta_{cd,j} = \frac{\theta_{cx,j} - \theta_{c,j}}{2}$, $\beta_{sl,j} = \frac{\theta_{sx,j} + \theta_{s,j}}{2}$, $\beta_{cl,j} = \frac{\theta_{cx,j} + \theta_{c,j}}{2}$.

In our climatic context, the time trend variable is a coarse proxy, while GHGs radiative forcing (AGGI index) is a causal mechanism. Yet, consistent with Philippon (2022), the time trend proxy might convey information about the underlying force driving global GHG levels, i.e., global economic growth.

Hence, the common level parts (10) and (11) capture the underlying common trend, and potentially yield a measure of cumulated GHGs over time, i.e., their stock level. The common difference parts (8) and (9) measure the deviation of GHGs dynamics from a constant-pace time path, and, therefore, their accelerations and decelerations over time. In both cases, Fourier-transformed variables are considered, enabling effective modeling of potential non-linearities in their impact.

Keeping into account the common normalization of the AGGI and the time trend variable, the level and difference components (nearly) yield the first and second principal components for any couple of Fourier transformed series of the type $\sin(2\pi j x_t^*)$ and $\sin(2\pi j\frac{t}{T})$ or $\cos(2\pi j x_t^*)$ and $\cos(2\pi j\frac{t}{T})$, $j = 1, \dots, 3$. The latter result is exact only after standardizing the transformed regressors to ensure they have the same variance. This implies that the identifiable directions are the linear combinations of the common variables, rather than the variables themselves. Therefore the estimable parameters are $\beta_{sd,j}$, $\beta_{cd,j}$, $\beta_{sl,j}$, $\beta_{cl,j}$.

In the more general and likely case, where both the difference and level components contain signal, i.e., where extreme weather developments depend not only on GHG acceleration and deceleration relative to the constant-pace trend, but also on their accumulation over time (their stock), one can expect

$$\beta_{sd,j} \neq 0 \text{ and/or } \beta_{cd,j} \neq 0 \text{ and } \beta_{sl,j} \neq 0 \text{ and/or } \beta_{cl,j} \neq 0, \tag{13}$$

i.e.,

$$\theta_{sx,j} \neq \theta_{s,j} \text{ and/or } \theta_{cx,j} \neq \theta_{c,j} \text{ and } \theta_{sx,j} \neq -\theta_{s,j} \text{ and/or } \theta_{cx,j} \neq -\theta_{c,j}, \tag{14}$$

for some $j = 0.5, 1, \dots, 3$. Therefore, the model in (12), after rearranging, can be rewritten in terms of a model for the quasi-differences

$$y_{n,t} = \sum_{j=0.5}^{j^*} (\beta_{sd,j} + \beta_{sl,j}) \left(\sin(2\pi j x_t^*) - \frac{(\beta_{sd,j} - \beta_{sl,j})}{(\beta_{sd,j} + \beta_{sl,j})} \sin(2\pi j \frac{t}{T}) \right) + \sum_{j=0.5}^{j^*} (\beta_{cd,j} + \beta_{cl,j}) \left(\cos(2\pi j x_t^*) - \frac{(\beta_{cd,j} - \beta_{cl,j})}{(\beta_{cd,j} + \beta_{cl,j})} \cos(2\pi j \frac{t}{T}) \right) + \epsilon_{n,t}. \tag{15}$$

On the other hand, if stocks do not matter, i.e., $\beta_{sl,j} = 0$ and $\beta_{cl,j} = 0$, and, therefore, $\theta_{sx,j} = -\theta_{s,j}$ and $\theta_{cx,j} = -\theta_{c,j}$, $j = 0.5, 1, \dots, 3$, the common level component drop off the model yielding the exact difference model

$$y_{n,t} = \sum_{j=0.5}^{j^*} \beta_{sd,j} sd_{jt} + \sum_{j=0.5}^{j^*} \beta_{cd,j} cd_{jt} + \epsilon_{n,t}. \tag{16}$$

The estimation strategy we follow, i.e., machine-driven general to specific reduction (GETS) through Autometrics (Hendry et al., 2008), overcomes the potential multicollinearity problem plaguing the original panel model specification in (5), yet avoiding the direct estimation of the rotated specification in (7), and, therefore, changing the definition of the conditioning regressors, or of its difference or quasi-difference forms. Autometrics effectively discovers and estimates the difference or quasi-difference models in (15) and (16) because of how the automated GETS algorithm handles near-collinearity. When perfect collinearity is present, Autometrics drops the offending regressor(s). However, under high but imperfect collinearity, estimation proceeds, and statistical tests, such as t-tests, F-tests, information criteria, and encompassing tests, drive model reduction. Since collinear regressors tend to have weak individual significance, they are often removed during the reduction process. A key advantage of machine-based GETS over human-based GETS is Autometrics' use of multiple reduction paths, which mitigates path dependence. If collinearity destabilizes one path, another may retain a different subset of regressors.

Crucially, Autometrics does not eliminate variables because they are collinear; it eliminates them only when they fail statistical tests. As a result, even regressors that are nearly linear combinations of one another may survive along different search paths. In the final union model, constructed by retaining all variables that survive at least one admissible path, both regressors may appear, even if they are nearly collinear. When one variable is retained with a positive coefficient in one path and the other with a negative coefficient in another, the resulting union model behaves like a quasi-difference. Autometrics does not explicitly construct such linear combinations. Instead, the reduction process naturally leaves behind variables that represent the only statistically identifiable direction in the regressor space. If the quasi-difference is the identifiable signal in the data, it will be retained. Thus, the quasi-difference model arises because near-collinearity restricts identification to a single linear combination of the regressors, and Autometrics' multi-path GETS procedure preserves the regressors that survive along that identifiable direction. See the Online Appendix for further discussion of specification issues.

In light of the above discussion, upon estimation of the specification in (5), we can use a Wald test to assess the null hypothesis of non-evolving extreme weather conditions (Test 1), i.e.,

$$H_0 : \theta_{sx,j} = \theta_{sx,n,j} = \theta_{cx,j} = \theta_{cx,n,j} = \theta_{s,j} = \theta_{s,n,j} = \theta_{c,j} = \theta_{c,n,j} = 0,$$

and $j = 0.5, 1, 2, 3$. Rejecting the null hypothesis in Test 1 yields confirmation of the evidence for evolving extreme weather behavior documented by the augmented KPSS tests, also within our extended framework, which allows for direct conditioning on GHGs.

Moreover, a test for the null hypothesis of the "exact difference model" for the common components (Test 2) is

$$H_0 : \theta_{sx,j} = -\theta_{s,j} \text{ and } \theta_{cx,j} = -\theta_{c,j} = 0, \tag{17}$$

$j = 0.5, 1, 2, 3$.

Rejecting the null hypothesis in Test 2 points to the relevance of the "quasi-difference model", i.e., of both the flow and stock dimensions of GHG forcing for the determination of extreme weather behavior, therefore establishing a conditional statistical association between extreme weather behavior and GHG emissions. Rejecting the null hypothesis in Test 2 is also consistent with rejecting it in Test 1, as it implies establishing a trend or evolving behavior in extreme weather conditions, yet driven by common sources.

Yet, rejecting the null hypothesis in Test 2 might have much stronger implications, adding some support for a causal interpretation. This follows from the fact that, in our model, GHG radiative forcing is measured on a global scale and, therefore, is plausibly exogenous or at least not contemporaneously affected by extreme weather events localized in Europe. Extreme weather in Europe, in theory, can impact global GHGs through various channels, such as energy system stress, due to increased use of fossil fuels to face spikes in energy demand following heatwaves or cold snaps, wildfires that directly release CO_2 and reduce forests that normally absorb carbon, or through infrastructure damage caused by floods, storms, and wildfires, which boost the use of cement, steel, and energy-all carbon-intensive- during reconstructions. Yet, within the time span considered in the study, it is unlikely that these phenomena are significant contributors to the global trend in GHG emissions. Moreover, our results are established through an automated procedure that allows us to draw robust conclusions to alternative trend specifications and reduction paths, and the "quasi-difference" model emerges as a strong regularity across all the extreme weather typologies investigated. Hence, although we do not provide formal testing for a causal link between anthropogenic GHG radiative forcing and extreme weather episodes, we highlight that our physical exogeneity and directional asymmetry conjecture, as well as considerations of modeling strategy robustness, might help bridge the gap toward a causal interpretation.

Table 2
Common drivers of evolving extreme weather conditions across countries.

	Dependent variable							
	E3CI	Max Temp	Min Temp	Drought	Wind	Precipitation	Fire	Hail
θsx05	2.677	−2.437	38.679	–	24.554	–	–	−21.780
	(0.992)	(0.569)	(4.342)		(6.043)			(3.783)
θsx1	−2.616	−6.180	0.115	–	−7.239	–	0.392	–
	(0.606)	(1.163)	(0.045)		(1.867)		(0.059)	
θsx2	0.343	−0.382	–	1.438	−1.628	–	1.909	–
	(0.151)	(0.137)		(0.285)	(0.457)		(0.324)	
θsx3	−0.269	–	–	−0.365	−0.165	0.133	−0.402	−0.403
	(0.052)			(0.051)	(0.063)	(0.023)	(0.066)	(0.078)
θcx05	5.903	10.129	2.704	−5.430	9.387	–	–	4.164
	(1.122)	(2.178)	(0.467)	(0.872)	(2.192)			(0.574)
θcx1	–	−3.644	15.901	2.770	9.228	−0.748	–	−9.400
		(0.734)	(1.692)	(0.225)	(2.428)	(0.122)		(1.429)
θcx2	0.089	−1.452	2.215	–	–	–	0.539	–
	(0.029)	(0.252)	(0.232)				(0.092)	
θcx3	0.151	–	0.284	1.133	–	−0.231	0.712	−0.424
	(0.035)		(0.053)	(0.101)		(0.043)	(0.112)	(0.086)
θs05	−2.825	–	−41.655	6.607	−28.299	−1.825	3.718	21.132
	(0.986)		(4.801)	(0.540)	(6.897)	(0.286)	(0.719)	(3.852)
θs1	3.022	6.869	–	–	7.432	–	–	–
	(0.640)	(1.234)			(1.886)			
θs2	−0.326	0.649	–	−1.347	1.905	–	−1.990	−0.322
	(0.164)	(0.174)		(0.280)	(0.538)		(0.334)	(0.038)
θs3	0.107	–	–	–	0.326	−0.102	–	0.231
	(0.048)				(0.098)	(0.022)		(0.061)
θc05	−6.073	−11.056	−2.499	5.358	−9.464	−0.078	−0.224	−3.796
	(1.118)	(2.188)	(0.482)	(0.863)	(2.192)	(0.008)	(0.044)	(0.536)
θc1	–	2.675	−17.154	–	−11.006	–	1.731	9.215
		(0.823)	(1.904)		(2.851)		(0.320)	(1.454)
θc2	–	1.439	−2.690	0.662	−0.450	−0.160	–	–
		(0.192)	(0.275)	(0.054)	(0.124)	(0.024)		
θc3	−0.194	–	−0.499	−0.851	–	0.158	−0.638	0.211
	(0.036)		(0.059)	(0.088)		(0.033)	(0.103)	(0.069)
Constant	0.046	1.690	1.851	−3.958	2.386	1.138	−2.606	0.282
	(0.035)	(0.401)	(0.336)	(0.325)	(0.565)	(0.173)	(0.453)	(0.154)
R^2	0.381	0.601	0.278	0.150	0.093	0.117	0.323	0.169
$\bar{R}^2$	0.372	0.598	0.270	0.142	0.083	0.109	0.315	0.164

This Table reports the regression coefficients for the common components across countries of the panel data model in (6). OLS estimation is performed through Autometrics, the automated general-to-specific model reduction strategy by Hendry et al. (2008). The model reduction analysis is carried out for the E3CI index and for each of its components separately. Heteroskedasticity-consistent standard errors are shown in parentheses.

3.2. Empirical results

The order of the trigonometric polynomial $j^* = 3$ in (5) is motivated by climatological arguments and set to allow the trend component to describe fluctuations with periodicity larger than 14 years ($P^* = \lfloor T/j^* \rfloor = 14.3$, where $T = 43$), avoiding potential contaminations from natural oscillators which follows shorter periodicty, such as ENSO (2 to 7 years), NAO (8 to 10 years), and solar activity (about 11 years). This threshold allows discrimination between potential changes in the weather indicators driven by short-periodic natural phenomena, implicitly modeled by the disturbance term $\epsilon_{n,t}$, and those driven by human activity (GHGs) and long-periodic natural oscillations. For instance, the AMO may mask or exaggerate the contribution of the warming trend, depending on its phase, thereby affecting the underlying weather conditions as well (Wu et al., 2011; Swanson et al., 2009). Moreover, the stationarity tests in Table 3 show little difference between the null hypotheses of second- and third-order nonlinear trend stationarity, suggesting against selecting a model of order higher than three.

As $N = 40$, the starting specification in (5) counts 680 parameters and can only be estimated using machine-based GETS model reduction. The analysis is conducted for the E3CI index and its components separately. We report the final econometric models in Tables 2 and 4. In particular, Table 2 reports the final specification for the common components across countries, while Table 4 presents the final specification for the components accounting for cross-country heterogeneity. We report Heteroskedasticity-consistent standard errors in all cases.

As shown in Tables 2 and 4, the common component is strongly dominant over the idiosyncratic component, consistent with the global nature of climate change and the potential additional contribution of natural oscillators with long periodicity and global impact. This finding aligns with Bilal and Kanzig (2024) and Cassola et al. (2025). In fact, for any of the weather indicators, most of the retained regressors are trigonometric polynomials building up the common part. For instance, for extreme maximum temperature, out of the 16 retained regressors in the final specification, 12 (4) contribute to the common (idiosyncratic) part, i.e., the ratio of common over total parameters is 0.75. Similar findings hold for the other indicators, but for precipitations and wildfires,

Table 3
Wald tests.

	Test 1	Test 2
E3CI	26.789 [0.000]	25.985 [0.000]
	F(20,1694)	F(7,1694)
Max Temp	128.280 [0.000]	21.696 [0.000]
	F(15,1704)	F(5,1704)
Min Temp	32.819 [0.000]	37.405 [0.000]
	F(18,1701)	F(5,1701)
Drought	17.645 [0.000]	43.503 [0.000]
	F(16,1703)	F(3,1703)
Wind	8.160 [0.000]	3.850 [0.001]
	F(19,1700)	F(6,1700)
Precipitation	12.849 [0.000]	18.814 [0.000]
	F(16,1703)	F(2,1703)
Fire	47.760 [0.000]	43.503 [0.000]
	F(21,1698)	F(3,1703)
Hail	20.475 [0.000]	15.530 [0.000]
	F(11,1708)	F(5,1708)

This Table reports the results of the Wald tests for the null hypothesis of no evolving extreme weather conditions (Test 1), and for the null hypothesis of exact difference model specification (Test 2).

Table 4
Heterogeneities of evolving extreme weather conditions across countries.

Dependent variable													
E3CI		Max Temp		Min Temp		Drought		Wind		Precipitation		Fire	
θcos05xIS	0.174	θcos05tMT	−0.294	θsin3xAL	−0.171	θsin1tIT	0.205	θsin3xSI	0.138	θsin1xLT	0.137	θsin05tIE	−0.685
	(0.026)		(0.136)		(0.060)		(0.082)		(0.053)		0.043		(0.095)
θcos05xIE	0.107	θcos05tSI	−0.347	θsin3xMK	−0.117	θsin1tMK	0.247	θcos05xCY	−0.097	θsin1xLU	0.126	θsin05tMT	0.383
	(0.039)		(0.118)		(0.049)		(0.110)		(0.048)		0.034		(0.080)
θcos05xNO	0.115	θcos05tSE	0.223	θcos05xLV	−0.132	θsin3tIS	0.237	θcos05xEL	−0.098	θcos05xFR	0.083	θintAD	−0.344
	(0.030)		(0.089)		(0.051)		(0.082)		(0.034)		0.026		(0.047)
θsin05tAT	−0.076	θcos1tIS	−0.325	θsin05tLV	0.101	θcos05tAL	0.280	θcos05xMK	−0.115	θcos05xMT	0.134	θintAT	−0.354
	(0.025)		(0.088)		(0.043)		(0.097)		(0.048)		0.074		(0.043)
θcos05tFI	0.114			θcos05tCY	0.195	θcos05tEL	0.223	θcos2xUK	−0.122	θcos05xCH	0.114	θintEE	−0.273
	(0.036)				(0.076)		(0.080)		(0.047)		0.037		(0.046)
θcos05tSE	0.113			θcos05tEE	−0.120	θcos05tME	0.183	θcos1tCZ	−0.128	θcos1xLU	0.099	θintFI	−0.331
	(0.029)				(0.052)		(0.092)		(0.059)		(0.051)		(0.040)
θsin05tCH	−0.109			θcos1tUK	0.100					θsin1tMK	−0.088	θintIS	−0.716
	(0.022)				(0.041)						(0.041)		(0.036)
θintFI	−0.092									θsin3tLU	0.101	θintNO	−0.524
	(0.023)										(0.040)		(0.030)
θintIS	−0.163											θintSE	−0.350
	(0.016)												(0.035)
θintIE	−0.127											θintCH	−0.543
	(0.022)												(0.041)
θintNO	−0.109											θintUK	−0.352
	(0.017)												(0.052)
θintSE	−0.083												
	0.019												

This Table reports the regression coefficients for the components accounting for cross-country heterogeneity of the panel data model in (6). OLS estimation is performed through Autometrics, the automated general-to-specific model reduction strategy by Hendry et al. (2008). The model reduction analysis is carried out for the E3CI index and for each of its components separately. Heteroskedasticity-consistent standard errors are shown in parentheses.

for which the ratio is, however, larger than 0.5. The same holds for the E3CI index as well, which, not surprisingly, aggregates the various components and exhibits the most profligate final specification. The results align with previous evidence on global temperatures from Morana and Sbrana (2019) and Estrada et al. (2013a,b).

Moreover, the discovery and estimation of the quasi-difference specification is pervasive across indicators, and can easily noted from the retention of pairs of trigonometric components in the AGGI and time variables, i.e., $\sin(2\pi j x_t^*)$ and $\sin(2\pi j \frac{t}{T})$, or $\cos(2\pi j x_t^*)$ and $\cos(2\pi j \frac{t}{T})$, $j = 1, \dots, 3$, entering the specification with similar magnitudes, yet with opposite signs. For instance, in Table 2, for the E3CI index, one can note $\hat{\theta}_{sx,05} = 2.667$ and $\hat{\theta}_{s,05} = -2.825$, or $\hat{\theta}_{cx,05} = 5.903$ and $\hat{\theta}_{c,05} = -6.073$, among the various occurrences. Similar evidence can be noted for all the E3CI index components. In Table 3, we present the results of the Wald tests for the null hypothesis of non-evolving weather conditions (Test 1) and the null hypothesis of the exact difference model (Test 2), which is again equivalent to the null of non-(common) trend behavior in extreme weather conditions. The null hypothesis is decisively rejected in both cases, reinforcing the conclusion that underlying extreme weather patterns are changing and are at least partly driven by

a common factor. In this respect, as already noted, the discovery of the quasi-difference model is consistent with the relevance of both trend and cyclical GHGs for the determination of extreme weather behavior in Europe, yet with the caveat that we do not formally establish a causal association between the two phenomena.

As shown in Table 4, Nordic countries, including Iceland, Norway, Finland, Sweden, as well as Ireland and Switzerland, are identified as outlying countries relative to the common overall extreme weather dynamics described by the E3CI index reported in Table 2. The E3CI components can gauge further insights into countries' heterogeneity. For instance, Iceland and Sweden are outliers based on extreme maximum temperatures and wildfire indicators. Iceland is also selected based on the drought component. Norway, Finland, Ireland, and Switzerland are selected based on the wildfire indicator, and Switzerland is also selected based on the extreme precipitation component. Many other countries are outliers according to one or more E3CI components. Among the Northern Europeans, Latvia, Estonia, and Lithuania; among the Southern Europeans, Malta, Cyprus, Andorra, Greece, Italy, Slovenia, Montenegro, Albania, and North Macedonia. Among Central/Northern European countries, Czechia, France, and the UK. Hence, although a dominant large-scale driver shapes extreme weather across Europe, distinct regional mechanisms lead to divergent developments in Northern and Southern countries. This pattern aligns with well-documented atmospheric dynamics – most notably jet-stream variability – which generate dipole structures in air pressure, temperature, precipitation, and drought between northwestern and southeastern Europe (Xu et al., 2024).

The trend components reported in Fig. 2 are obtained by averaging the fitted trends from the panel data regression in (5). Visual inspection suggests that cyclical variability predominates over trend variability across all extreme weather series. Since only the trend component can be at least partially attributed to anthropogenic climate change, using raw extreme-weather series in economic assessments may not be optimal. In this respect, contamination from short-term or cyclical fluctuations acts as additive observational noise, biasing downward the estimated impact parameters. By instead relying on the estimated trend components, our analysis is shielded from this drawback and therefore provides a more accurate evaluation of the economic costs of climate change.

4. Modeling the economic effects of extreme weather

We perform a comprehensive assessment of the economic impact of evolving extreme weather, focusing on real GDP growth (level and per capita), as well as its sectoral gross Value-Added decomposition. We also assess its transmission mechanisms, distinguishing between demand-side and supply-side channels. Specifically, the supply-side variables considered in the study are real GDP per hour worked and per person employed, total factor productivity, hours worked, the number of persons employed, and the real capital stock. The demand-side variables are the real GDP expenditure components, namely private consumption and investment, government expenditure, and net exports. Refer to the Online Appendix for further details on the data.

In the empirical analysis, we use a dynamic panel regression with fixed-country and time effects. The baseline regression is

$$\Delta y_{j,t} = \alpha_j + \lambda_t + \beta \Delta y_{j,t-1} + \gamma \widehat{E3CI}_{j,t} + u_{j,t}, \tag{18}$$

where $\Delta y_{j,t}$ is the percent change in the real per capita GDP in country j in period t or the rate of growth for any of the variables indicated above, $\widehat{E3CI}_{j,t}$ is the E3CI index fitted component for country j in period t obtained from (5), α_j is the country fixed effect, λ_t is the time fixed effect, and $u_{j,t}$ is an i.i.d. residual.

The E3CI index includes seven components, namely extreme maximum and minimum temperatures, wind speed and precipitation, droughts, hail, and wildfires. In regression (19), we assess the impact of worsening extreme weather conditions by considering each component separately. Our additional econometric model is

$$\Delta y_{j,t} = \alpha_j + \lambda_t + \beta \Delta y_{j,t-1} + \gamma_i \widehat{EWI}_{i,j,t} + u_{j,t} \quad i = 1, \ldots, 7, \tag{19}$$

where, rather than the fitted composite E3CI index, we use each of its seven fitted components as conditioning variables. Hence, $\widehat{EWI}_{i,j,t}$ is the ith E3CI index component in country j in period t.

Despite their simplicity, the dynamic panel specifications in (18) and (19) yield a reliable assessment of the impact of evolving extreme weather conditions on economic activity, as they employ country and time effects to control for residual variability that potentially omitted conditioning variables may contribute. They are estimated by FE OLS with robust SE, within an Autometrics (Hendry et al., 2008) framework to specify country- and time-fixed effects according to statistical significance and enhance estimation efficiency.

In our context, where $N = 40$ and $T = 43$, the Nickell bias is likely to be negligible given the sizable temporal dimension (Hausman and Pinkovskiy, 2017), and FE OLS is expected to deliver accurate estimates. Yet, for robustness, we implement the state-of-the-art bias-corrected estimator by Breitung et al. (2022), which, as demonstrated in Monte Carlo simulations, outperforms the Arellano-Bond GMM estimator. Moreover, by conditioning on the extreme-weather trend components driven by radiative forcing, we avoid potential downward bias arising from unrelated short-periodic natural phenomena and observational noise. Yet, the trend components are estimated, potentially exposing our estimates to gene-rated regressor bias. For robustness, we then implement the Anderson-Hsiao IV estimator, which, in our case ($N \cong T$), is also superior to the Arellano–Bond GMM estimator in both asymptotic and small-sample properties (Hsiao and Zhang, 2015).

4.1. Controlling for cross-country heterogeneity

The symmetric models in (18) and (19), by averaging across countries, may dilute potential heterogeneities arising from varying attitudes toward environmental policy, institutional quality, income levels, and geographical factors. To control for their potential mitigation or enhancement of the adverse effects of climate change, we also consider their asymmetric versions. We then have

$$\Delta y_{j,t} = \alpha_j + \lambda_t + \beta \Delta y_{j,t-1} + \gamma_p \left(\widehat{E3CI}_{j,t} \times I^+_{j,t} \right) + \gamma_m \left(\widehat{E3CI}_{j,t} \times I^-_{j,t} \right) + u_{j,t}, \tag{20}$$

$$\Delta y_{j,t} = \alpha_j + \lambda_t + \beta \Delta y_{j,t-1} + \gamma_p \left(\widehat{EWI}_{i,j,t} \times I^+_{j,t} \right) + \gamma_m \left(\widehat{EWI}_{i,j,t} \times I^-_{j,t} \right) + u_{j,t} \quad i = 1, \dots, 7, \tag{21}$$

where $I^+_{j,t}$ ($I^-_{j,t}$) is the indicator variable taking unitary value in case country j at time period t shows an above (below) time-t cross-sectional mean value for the given policy variable of interest and zero otherwise, i.e., if country j at time period t is a relatively virtuous or leader (non-virtuous or laggard) country according to the specific policy criterion considered. Specifically, our policy control variables include a country's level of implementation of mitigation and adaptation policies, the quality of its institutions, its level of wealth, and its climate zone. Regarding adaptation policy, our measures include the Notre-Dame Global Adaptation Index (ND-GAIN) and its two components: readiness and vulnerability. Our mitigation policy indicator is the Germanwatch Climate Change Performance Index (CCPI). Our indicator of institutions' quality is based on whether a country operates as a market economy aligned with (virtuous) EU standards. Wealth is measured by the level of real per capita GDP, and climate zones are defined by average land temperature, latitude, and longitude. For the latter two cases, the indicator $I^+_{j,t}$ ($I^-_{j,t}$) takes a unitary value if a given country is a Northern or Western European country (a Southern or Eastern European country). Refer to the Online Appendix for further details on the data for the above nine indicators.

4.2. Robust estimation through model averaging

We provide a specification-robust assessment of the climate change impact on economic activity, by exploiting the empirical distribution of the estimated γ, and γ_i, $i = p, m$ impact parameters. For instance, concerning the effects of deteriorating overall extreme weather conditions on GDP growth, nineteen impact parameter estimates are available, i.e., one from the symmetric specification (18) and eighteen from the nine asymmetric specifications (20). By holding these estimates as the generic realizations of the variable γ_{MA}, and denoting its cumulative distribution function as $G(\gamma_{MA})$, its τth quantile is

$$Q^m = \inf \left\{ \gamma_{MA} : G_j(\gamma_{MA}) \geq \tau \right\}, \tag{22}$$

i.e., the minimum value of γ_{MA} from amongst all those values whose cumulative distribution function value exceeds m, and $\tau = 0.25$, 0.5, 0.75 in our analysis. The lowest quantile $\tau = 0.25$ is the first quartile, i.e., the smallest value, such that there is a 25% (or greater) probability that the estimated impact parameter will be larger than the value. Symmetrically, the upper quantile $\tau = 0.75$ yields the third quartile. The median corresponds to $\tau = 0.5$.

We perform robust model averaging estimation, as described above, for the responses of level and per capita real GDP growth, as well as for sectoral Value-Added growth, and any of the supply-side and demand-side variables.

We also consider broader cross-sectional sets. For instance, the first extended set jointly evaluates the impact parameters obtained from level and per capita GDP growth, as well as sectoral Value-Added growth, which yields $5 \times 19 = 95$ impact parameter estimates. The second one includes the supply-side variables ($6 \times 19 = 114$ estimates). The third one contains the demand-side variables ($4 \times 19 = 76$ estimates), while the fourth one includes all the previous variables, and provides information on the climate change effects on an implied economic activity broad index. We carry out this latter operation by keeping separate the sets of γ_i, $i = p, m$ impact estimated parameters for each control variable (16 parameters) to obtain robust indications about the role played by geographical factors, environmental policy, institutional, and economic development in mitigating or enhancing climate change economic effects. These model averaging operations are conducted for the overall E3CI index and each of its components, providing a robust yet detailed assessment of the economic costs associated with evolving extreme weather conditions.

5. Evidence on extreme weather economic impact

Our analysis begins with an assessment of the impact of deteriorating overall extreme weather conditions on level and per capita real GDP growth, and on sectoral Value-Added growth. Table 5 reports the E3CI index impact estimated from the symmetric and asymmetric models in (18) and (20). Table 6 presents complementary evidence for the various E3CI components from the symmetric models in (19). Detailed results for the asymmetric models in (21) are reported in Table A2–A6 in the Online Appendix. Moreover, Fig. 5 displays results for the model averaging analysis carried out variable-by-variable using the point estimates from the symmetric and asymmetric models in (18)–(20) and (19)–(21). Table 7 reports the median and other quartile values displayed in Fig. 5, as well as the implied annual impact of deteriorating extreme weather conditions on the level and per capita real GDP growth.

Columns list the endogenous variables. Hence, for instance, the results reported in the first row of the column headed GDP per capita in Table 5 are for the estimated impact parameter γ in (18), i.e., for the mean effect of deteriorating overall extreme weather conditions. The results reported in the following two rows are for the asymmetric impact parameters γ_p and γ_m in (20), where the fitted E3CI index is interacted with the dummy variable controlling for the relative level of adaptation, i.e., above or below average. The subsequent pairs of rows report similar results for the other controls, from the readiness and vulnerability components of the adaptation index through the geographical controls. The second column, headed "GDP", reports results for the symmetric and asymmetric regressions when the dependent variable is real GDP growth, and the other columns in Table 5 present similar results for the other variables.

Table 5
GDP and Sectoral Value Added growth rates, $\widehat{E3CI}$ impact.

	GDP per capita	GDP	Agriculture	Industry	Service
FE	−1.387**	−1.276***	−1.189	−3.470***	−5.657***
	(0.628)	(0.404)	(1.714)	(0.986)	(1.140)
Adaptation					
More	−1.274*	−1.436***	0.191	−3.154**	−6.175***
	(0.752)	(0.463)	(2.056)	(1.194)	(1.127)
Less	−1.960**	−1.337**	−2.631	−4.473***	−4.904***
	(0.850)	(0.656)	(2.566)	(1.540)	(1.540)
Readiness					
More	−1.353**	−1.520***	0.035	−3.309***	−6.317***
	(0.647)	(0.379)	(1.760)	(1.149)	(1.128)
Less	−1.951**	−1.288*	−3.143	−4.027**	−4.839***
	(0.871)	(0.748)	(2.765)	(1.633)	(1.607)
Vulnerability					
Less	−1.388*	−1.539***	0.728	−3.684***	−5.944***
	(0.688)	(0.460)	(2.286)	(1.156)	(1.328)
More	−1.988**	−1.153*	−4.112*	−3.984**	−4.938***
	(0.831)	(0.653)	(2.364)	(1.676)	(1.359)
Mitigation					
More	0.220	0.607	0.392	−3.459	−6.379***
	(1.047)	(0.937)	(3.510)	(2.580)	(1.715)
Less	−0.850	−0.029	−5.279*	−5.530**	−7.347***
	(1.037)	(0.847)	(2.699)	(2.149)	(1.661)
Institutions					
Better	−1.221**	−1.141***	−1.423	−3.272***	−5.281***
	(0.585)	(0.404)	(1.797)	(0.943)	(1.120)
Worse	−2.956	−2.771	1.010	−5.693	−9.021***
	(2.481)	(2.035)	(3.533)	(3.509)	(2.036)
Income					
Above	−0.593	0.369	0.685	4.921	−5.871***
	(2.292)	(1.536)	(1.791)	(4.313)	(1.642)
Below	−1.455**	−1.437***	−1.373	−4.246***	−5.640***
	(0.591)	(0.395)	(1.842)	(1.127)	(1.159)
Temperature					
Above	−0.887*	−1.425**	−4.530	−3.739***	−5.038***
	(0.475)	(0.610)	(3.086)	(1.236)	(1.531)
Below	−1.664**	−1.201**	0.429	−3.343***	−5.953***
	(0.794)	(0.469)	(1.957)	(1.053)	(1.153)
Geography					
West	−0.835	−1.393***	0.380	−2.792***	−6.049***
	(0.685)	(0.461)	(2.123)	(0.903)	(1.282)
East	−2.222**	−1.103*	−3.150	−4.410***	−5.059***
	(0.898)	(0.626)	(2.533)	(1.468)	(1.346)
North	−1.942**	−1.445***	0.622	−3.238***	−6.176***
	(0.791)	(0.457)	(2.000)	(1.013)	(1.084)
South	−0.587	−1.014*	−4.079	−3.873***	−4.697***
	(0.508)	(0.586)	(2.675)	(1.357)	(1.578)

This Table reports the E3CI index impact parameter, estimated from the symmetric and asymmetric models, on the growth rates of real per capita GDP, GDP, and the gross Value Added generated by the agriculture, industry, and service sectors. Heteroskedasticity-consistent standard errors are in parentheses. Specifically, we report the results from the FE OLS estimation of the symmetric models on the first row (FE). The results reported in the following two rows are for the FE OLS estimation of the asymmetric models, in which the fitted E3CI index is interacted with a dummy variable that controls for the relative level of adaptation (i.e., above or below average). The successive pairs of rows report similar results for the other controls, from the readiness and vulnerability components of the adaptation index through the geographical controls.

* Denote statistical significance at the 10% level.

** Denote statistical significance at the 5% level.

*** Denote statistical significance at the 1% level.

5.1. The effects of overall extreme weather conditions

As shown in Table 5 (first row, columns 1 and 2), deteriorating extreme weather conditions have a negative and significant impact on real GDP growth, which is robust to its level or per-capita definition. A unitary (one standard error) increase in the E3CI index yields a −1.4% (−1.3%) contraction in per capita (level) real GDP growth. The coefficient of determination of the regression is sizable ($R^2 = 0.55$), confirming that the included country and time effects are able to account satisfactorily for potentially omitted regressors in the growth equation.

Table 6
GDP and Sectoral Value Added growth rates, $\widehat{E3CI}$ components impact.

	GDP per capita	GDP	Agriculture	Industry	Service
Max Temp	−0.382*	−0.407***	−0.250	−0.821***	−1.135***
	(0.189)	(0.132)	(0.628)	(0.238)	(0.238)
Min Temp	1.672***	1.676***	2.212	2.208**	1.557**
	(0.467)	(0.368)	(2.961)	(1.006)	(0.642)
Drought	−1.191***	−0.112	−0.028	−1.254	−0.571
	(0.407)	(0.369)	(1.832)	(0.935)	(0.544)
Wind	−2.076	−3.105***	−2.186	−1.286	−3.664***
	(1.350)	(0.885)	(3.362)	(1.782)	(1.185)
Precipitation	−0.862	−2.447***	−1.032	−4.385**	−6.097***
	(1.392)	(0.849)	(5.211)	(2.098)	(1.173)
Fire	−0.877***	−0.319*	0.726	−1.246*	−1.554**
	(0.277)	(0.188)	(0.758)	(0.630)	(0.663)
Hail	1.446**	1.697***	1.447	4.121***	2.984***
	(0.659)	(0.536)	(2.120)	(1.243)	(0.565)

This Table reports the E3CI index's components impact parameter, estimated from the symmetric models, on the growth rates of real per capita GDP, GDP, and the gross Value Added generated by the agriculture, industry, and service sectors. Heteroskedasticity-consistent standard errors are in parentheses. The E3CI components are extreme maximum and minimum temperatures, droughts, extreme wind and precipitation, wildfires, and hail.

* Denote statistical significance at the 10% level.

** Denote statistical significance at the 5% level.

*** Denote statistical significance at the 1% level.

The comparison with the Anderson–Hsiao IV estimates (Table A1, Panel A, column 3, Online Appendix) reveals that the use of the fitted trend $\widehat{E3CI}$ component does not lead to generated regressor bias. As instruments, we use the AGGI index, its square, and the Global Living Planet Index (LPI, World coverage). We use the one-period lagged first differences of these variables as instruments. As shown in the Table, the Anderson–Hsiao IV estimator delivers point estimates of the γ parameter that are numerically very similar to the FE estimates and not statistically different, i.e. −1.5% (−1.0%). The misspecification tests fully validate IV estimation. The Kleibergen–Paap rk LM test statistic (K-P) rejects the null hypothesis of underidentification at all significance levels. Hence, the instruments are relevant and provide enough information to estimate the model consistently. Coherently, the Cragg–Donald Wald F-statistic (C-G) strongly rejects the null hypothesis of weak identification. Finally, the Sargan–Hansen J test, i.e., the overidentification test of all instruments, is largely passed, indicating that the instruments are uncorrelated with the error term and the model is correctly specified.

Secondly, the comparison with the Breitung et al. (2022) bias-corrected (BC) estimator (Table A1, Panel A, column 2) confirms that, as expected given our temporal sample size, Nickell bias is not an issue. The BC estimates are very similar to those of FE and IV, especially for per capita GDP, i.e., −1.5% (−2.1%). Also, the estimated inertia parameter β is strongly robust across specifications, at about 0.4, which, while moderate, still grants some persistence and temporal propagation to shocks and changes in extreme weather conditions. For instance, using the standard formula for a stationary AR-1 process, an overall extreme weather episode would lose approximately 50% (75%) of its impact after nine (eighteen) months on average. This estimated average dissipation rate is consistent with Usman et al. (2025), taking into account the uncertainty surrounding their IRFs.

Thirdly, the comparison with the point estimates obtained using the raw $E3CI$ index, rather than the fitted trend $\widehat{E3CI}$ index (Table A1, Panel B), confirms our expectation that contamination from short-periodic natural phenomena and observational noise may severely downward bias the impact of anthropogenic climate change. In fact, the magnitude of the effect is approximately half that estimated using the trend components, i.e., −0.8% (−0.8%). The BC estimates yield similar results, i.e. −0.7% (−0.9%). On the other hand, IV estimates align closely with the results reported for the fitted E3CI index, suggesting that using the raw E3CI index, rather than the fitted one, might lead to inconsistent and distorted estimation of the economic impact of extreme weather events.

Given the robustness of the results, we then employ the FE estimator and the fitted $\widehat{E3CI}$ index and $\widehat{EWI}$ components for the remainder of the analysis. In particular, the sectoral analysis (Table 5, columns 3 to 5) shows that the overall impact of deteriorating extreme weather conditions is negative for all sectors, more sizable for the services, i.e., (−5.7%) and industry (−3.5%) than agriculture (−1.2%), yet significant only for the former two sectors. The above findings align well with available evidence in Parker (2023), Usman et al. (2025) and Bodenstein and Scaramucci (2025). Climate change is not just an environmental issue. It is a macroeconomic disruptor. We dig further into the impact of extreme weather events and their transmission channels in the following Sections.

5.1.1. Cross-country heterogeneity

As shown in Table 5 (second row and below), implementing adaptation policies may help mitigate, but not eliminate, the adverse effects of climate change on economic activity. The impact on per capita GDP growth is weaker (stronger) for countries with higher (lower) adaptation and, therefore, higher readiness and lower vulnerability, i.e. −1.3% (−2.0%). The adaptation policy appears to focus on mitigating the adverse effects of climate change on agriculture and industry. For more (less) adapted countries, the point impact is +0.2% (−2.6%) for agriculture and −3.2% (−4.5%) for industry. The opposite holds for the service sectors, i.e., −6.2% (−4.9%), which also explains the lack of an asymmetric impact on GDP growth (−1.4%).

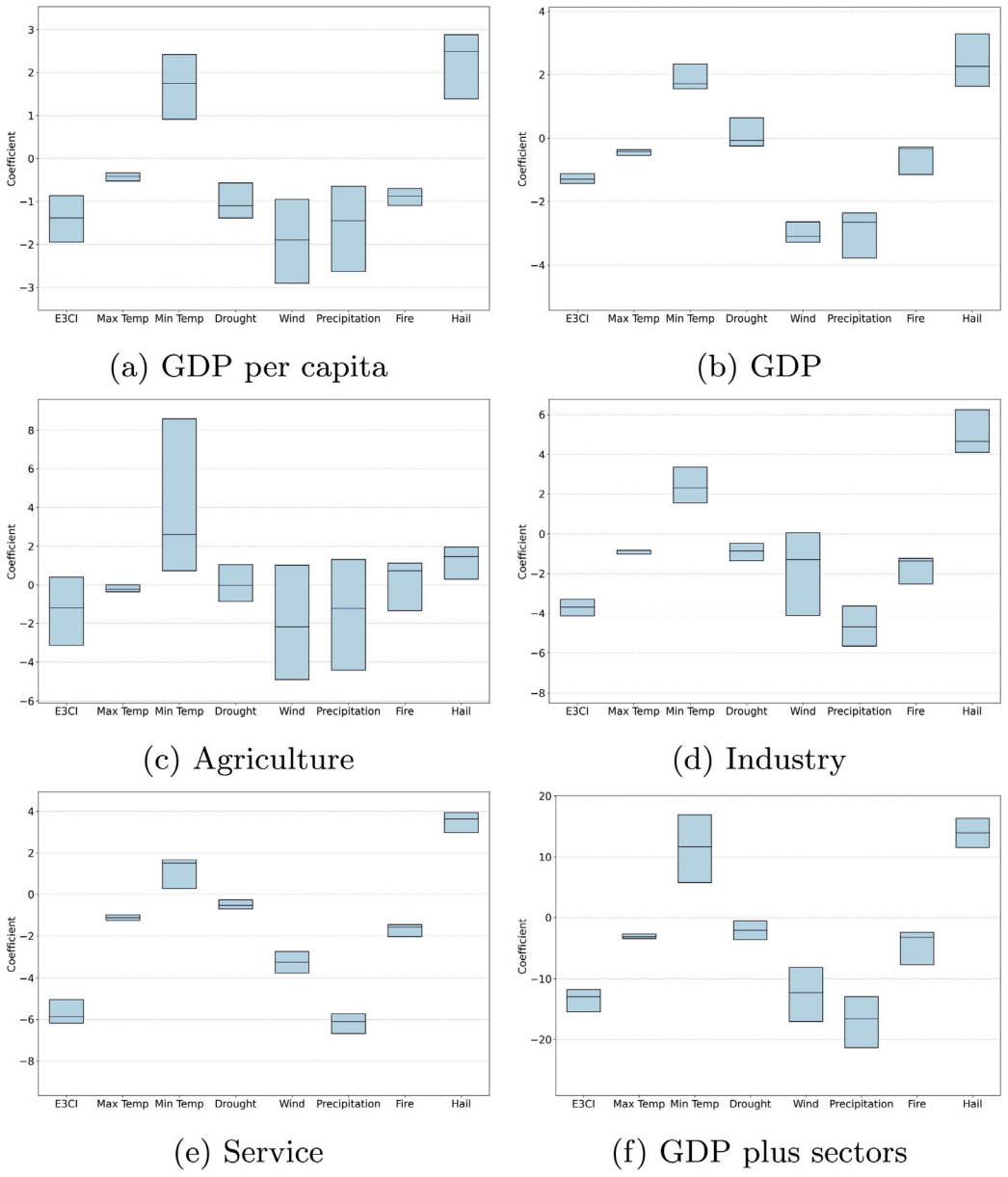

Fig. 5. GDP and Sectoral Value Added growth rates.
Note: The boxplots in this Figure report the results of the model averaging analysis carried out using the E3CI index and components' impact parameters, estimated from the symmetric and asymmetric models, on the growth rates of real per capita GDP, GDP, and the gross Value Added generated by the agriculture, industry, and service sectors. The E3CI components are extreme maximum and minimum temperatures, droughts, extreme wind and precipitation, wildfires, and hail. Plot (f) shows the averaging of results across the GDP and Value Added figures in plots (a) to (e) (GDP plus sectors).

Similarly, mitigation policies help cushion the adverse effects of extreme weather. Figures for countries with higher (lower) mitigation investment are +0.4% (−5.3%) for agriculture, −3.5% (−5.5%) for industry, and −6.4% (−7.4%) for services. Hence, unlike adaptation policy, mitigation policy appears to bring benefits across all sectors.

Better institutions (aligned with EU environmental standards) and relatively higher income also play a mitigation role. Figures for per capita GDP are −1.2% (−3.0%) and −0.6% (−1.5%) for countries with better (worse) institutions and higher (lower) affluence, respectively. Similar evidence holds for GDP growth. The institution's quality-mitigation effect is particularly sizable in the service sectors, i.e., −5.3% (−9.0%). The income-level mitigation effect is most relevant for the agriculture sector, i.e., +0.7% (−1.4%). Both are highly relevant to the industry sector, i.e., −3.3% (−5.7%) and +4.9% (−4.3%).

The above evidence can be easily rationalized. For instance, European citizens' concern about climate change is stronger in relatively higher-income countries, and therefore, public support for implementing environmental policies is also stronger (Baiardi and Morana, 2021). Alignment with EU institutional standards requires robust environmental legislation and the establishment of regulatory agencies responsible for oversight and enforcement, thereby promoting compliance with environmental standards. It unlocks financial support for sustainable infrastructure investments and the advancement of green policy initiatives (Canepa, 2025). In general, more affluent countries with better institutions can rely on better infrastructure, stronger governance, and greater financial resources, and therefore have a higher capacity to adapt and bear the short-term costs of mitigation policies (Fankhauser and McDermott, 2013).

The sectoral analysis also reveals distinct vulnerabilities by longitude and latitude. In this respect, the service sector is more affected in Northern and Western European countries. The agricultural and industry sectors are more affected in Southern and Eastern European countries. These results are consistent with the varying relative importance of the primary, secondary, and tertiary sectors in generating Value-Added in more and less advanced European countries. Figures for the service sector for Northern and Western (Southern and Eastern) European countries are −6.2% and −6.1% (−4.7% and −5.1%); for the agricultural sector, +0.6% and +0.4% (−4.1 and −3.2%); for the industry sector, −3.2% and −2.8% (−3.9% and −4.4%). Sectoral heterogeneity also explains the more substantial adverse effect on aggregate GDP growth for Northern and Western (than Southern and Eastern) European countries. Figures are −1.5% (−1.0%) for longitude, and −1.4% (−1.1%) for latitude.

In Fig. 5, the first boxplot (E3CI), in any of the plots (a) through (e), shows the outcome of the model averaging analysis carried out variable-by-variable using the point estimates of the $\widehat{E3CI}$ impact from the symmetric ($\hat{\gamma}$) and asymmetric models ($\hat{\gamma}_p$, and $\hat{\gamma}_m$) in (18)–(20). The first, second (median) and third quartiles reported therein provide complementary evidence on the size of the impact and its uncertainty, which is robust to specification choices. As shown in the boxplots, the results offer explicit confirmation of the adverse effect of climate change on economic activity, as not only the first quartile and the median, but also the third quartile, take negative values, indicating a relatively more substantial impact on the service sector than on the industry and agricultural sectors as well.

5.1.2. Extreme weather episodes

We further assess the impact of deteriorating extreme weather on economic activity by implementing our analysis component by component, i.e., by evaluating separately the effects of each of the seven E3CI components — extreme maximum and minimum temperatures, drought, extreme precipitation and wind, wildfires, and hail. The single-component analysis adds further insights into the origin of the overall effects uncovered using their aggregate, i.e., the E3CI index. We report the results for the symmetric models (19) in Table 6 and those for the asymmetric models (21) in Tables A2 through A6 in the Online Appendix. Moreover, Fig. 5 displays results for the model averaging analysis carried out variable-by-variable using the point estimates from the symmetric and asymmetric models in (18)–(20) and (19)–(21). In Table 7, we report the first, second (median), and third quartile values displayed in Fig. 5, as well as their implied expected yearly values. The latter figures are normalized point estimates, which yield the GDP growth responses to a typical year-to-year deterioration in extreme weather.

As shown in Table 6 (columns 1 and 2), the negative overall (E3CI) impact detected on GDP and value-added growth is accounted for by all categories of extreme weather events, but rising minimum temperatures and hail. The results also confirm that the adverse effect is generally strongest in the service sector.

Extreme wind and precipitation are the most damaging events. For wind, figures for GDP (per capita GDP) are −3.1% (−2.1%). The sectoral impacts are −3.7%, −1.3%, and −2.2% for services, industry, and agriculture, respectively. For precipitation, figures are −2.5% (−0.9%), and −6.1%, −4.4%, and −1.0%. These results align with the findings in Usman et al. (2025), which show that extreme rainfall significantly reduces macroeconomic growth, and with those in Kotz et al. (2022), which also show that the service sector is likely to be the most affected. Services rely heavily on infrastructure, mobility, and human interaction, making them particularly sensitive to disruptions from extreme weather events, especially power outages and transportation interruptions. Agriculture, while directly exposed to climate extremes, benefits from risk mitigation mechanisms such as insurance schemes and the Common Agricultural Policy (CAP), which buffer short-term losses (Devot et al., 2023). Notably, we find that storms tend to have a more substantial impact on agricultural output than floods, likely due to wind damage to crops and infrastructure. Industrial sectors exhibit greater resilience, supported by fixed capital investments and supply chain buffers. However, they remain vulnerable to production halts from power outages and logistical delays. We find that floods appear to have a more pronounced impact on industrial activity than storms, possibly reflecting the effects of facility inundation and disruptions to the transport network.

Consistent with Nguyen and Pienknagura (2024), we find a nonlinear effect of rising extreme temperatures on economic activity, adverse for maximum temperatures, and favorable for minimum temperatures. Figures for GDP are −0.4% and +1.7%. Similar results hold across sectors. Yet, the costs of rising maximum temperatures appear strongest for services (−1.1%), while the benefits of increasing minimum temperatures are for industry and agriculture (+2.2%). The latter pattern is consistent with the results in Burke et al. (2015), which show that total factor productivity exhibits a nonlinear relationship with temperature across all countries. Milder winters can be expansionary, reducing frost damage, extending growing seasons, lowering heating costs, and minimizing weather-related disruptions across sectors. In contrast, hotter springs and summers are contractionary, as elevated temperatures impair cognitive and physical performance, and increase heat-related morbidity and mortality. Temperature extremes, drought, and water scarcity weaken agricultural productivity and disrupt supply chains.

Regarding droughts, we find a negative, statistically significant impact on per capita GDP growth (−1.2%), suggesting that droughts may exert more persistent effects on individual welfare and productivity than on aggregate output. The effects are also more substantial for industry (−1.3%) and services (−0.6%), consistent with the potential adverse implications of water scarcity for hydroelectric energy generation, water-intensive manufacturing, and inland water transport. Similarly, wildfires impact more

per capita than level GDP growth (−0.9%), as well as services (−1.6%) and industry (−1.3%), through adverse effects on tourism (cancellations and infrastructure damage) and on energy and transport (grid disruptions and road closures during peak fire seasons). The modest positive impact on agriculture (+0.7%) is consistent with the literature highlighting the role of wildfires in facilitating land-use transitions that promote deforestation and subsequent agricultural expansion (Ascoli et al., 2021).

Finally, the impact of hail is positive and significant on GDP and its sectoral decomposition. Figure are +1.7% (+1.5%) for GDP (per capita GDP), and 2.3%, 4.1%, and 1.5% for service, industry, and agriculture. As previously noted, the E3CI hail component reveals a declining trend in the frequency of hail episodes over the past fifteen years. However, this reduction contrasts with a simultaneous increase in hailstorm intensity and destructive impact. The resulting positive economic figures are therefore puzzling. One plausible interpretation is that the decreasing frequency may be obscuring the rising severity of events. Moreover, these figures could reflect the growing effectiveness of insurance mechanisms and indemnity payments in cushioning agricultural losses (Devot et al., 2023), as well as the economic stimulus generated by reconstruction and adaptive investments. Increased demand for repair materials, resilient infrastructure, and emergency services – alongside heightened activity in insurance and logistics – may be contributing to short-term economic gains. This aligns with findings by Kotz et al. (2022) and Caggese et al. (2025), who emphasize that extreme events can produce ambiguous short-term effects, particularly when adaptation and insurance systems are robust.

At this stage, we do not discuss the implications arising from the cross-country heterogeneity analysis for the various extreme weather events, which we address in the Section devoted to drawing policy implications. While we acknowledge the importance of enriching the specification to account for asymmetric effects, the model averaging results reported in Fig. 5 suggest, however, that the detected patterns are robust to specification assumptions. We find confirmation of the negative (positive) point impacts by finding sign coherence in the first three quartiles of the impact parameters distribution for all events.

5.1.3. Predictions and comparative assessment

We conclude the event-based assessment, highlighting the implied predictions that emerge from our study in relation to the expected growth at risk inherent to a business-as-usual scenario for GHG emissions in Europe. In Table 7, Panel A, we report the median, and the first and third quartiles of the distribution of the estimated parameter reported in Fig. 5 (columns 1 to 3). We also report their rescaled magnitude to measure the yearly real GDP growth response to a typical (1 SD) change or worsening in (trend) extreme weather conditions. For instance, with reference to the E3CI index, the expected yearly median contraction in per capita GDP growth is approximately −0.08% (Q1: −0.11%; Q3: −0.05%). Figures for GDP growth are similar in terms of median impact, i.e., −0.07%, yet less dispersed (−0.08% to −0.06%). Similarly, for extreme wind, the annual median impact figures are −0.09% (−0.15%) for per capita GDP (GDP); for extreme precipitation, −0.05% (−0.10%); for wildfires, −0.09% (−0.03%); for droughts, −0.15% (−0.01%). The nonlinear median impact from extreme temperatures is +0.16 and −0.05% (+0.15 and −0.05%) for minimum and maximum temperatures, respectively. Finally, for hail, figures are +0.24% (+0.21%), where the already noted interpretation caveat applies.

In Table 7, Panels B and C, we also report key findings from complementary studies in the literature. Panel B presents the implied average yearly responses of GDP or GDP per capita to a *typical* worsening in extreme weather conditions, drawing on results from Felbermayr and Gröschl (2014, A), Orlov et al. (2020, B), García-León et al. (2021, C), Dietz and Lanz (2025, D), Cortés Arbués et al. (2024, E), Casey et al. (2023, F), Burke et al. (2015, G), Bodenstein and Scaramucci (2025, H), Natoli (2023, I), and Kahn et al. (2021, J). Because some studies report effects on GDP and others on GDP per capita, we compute the average of our estimated GDP and GDP per capita responses to obtain a unified measure of the overall impact on economic growth ($\bar{Q}_2$).

To facilitate comparison, we also harmonize across studies that differ in the type of climatic variable considered. Some studies estimate responses to increases in average temperatures (comparable to our E3CI-based estimates; studies D, F, G, I, J), while others focus on specific categories of extreme weather events, i.e., heatwaves, storms, heavy rainfall, and flooding. When multiple estimates are available for different event types, we report in the first row the average impact across phenomena (studies A, H). When a study examines only one type of extreme event, the average coincides with the single available estimate (studies B, C, E). For additional comparability, the last column reports the median response across all complementary studies. Comparing the first and last columns shows that our estimated losses are broadly consistent with the literature and close to the median values, although slightly below the median for droughts. Nevertheless, our estimates always fall within the minimum–maximum range reported in previous studies.

Panel C reports the implied average yearly responses of GDP or GDP per capita to an *atypical* deterioration in extreme weather conditions, defined as events above the 90th, 95th, or 99th percentile, depending on the study. Here we incorporate additional results from Felbermayr and Gröschl (2014, K), Bodenstein and Scaramucci (2025, L), Kimmich et al. (2025, M), Kotz et al. (2022, N), and Usman et al. (2025, O). Our implied responses are obtained by rescaling our parameter estimates using the largest annual change observed in the actual E3CI index and its components. For comparability, we apply the same harmonization strategy used for the typical-worsening case. As shown in Panel C, our estimated responses for atypical events also align well with the available literature, remaining slightly below the median impact reported in complementary studies, except in the case of heatwaves. In all cases, however, our estimates lie within the reported minimum-maximum range. Additional details on how we derive yearly average responses from the literature are provided in the Online Appendix.

6. Transmission mechanisms

Our analysis of climate change transmission mechanisms focuses on both demand and supply-side channels. On the supply side, we analyze total factor productivity and labor productivity (GDP per hour worked and per person employed), labor supply (hours

Table 7
Annual impact on GDP per capita and GDP across studies.

Panel A												
	GDP per capita						GDP					
	Coefficients			Annual impact			Coefficients			Annual impact		
	Q1	Q2	Q3	Q1	Q2	Q3	Q1	Q2	Q3	Q1	Q2	Q3
E3CI	−1.946	−1.387	−0.868	−0.11	−0.08	−0.05	−1.437	−1.288	−1.122	−0.08	−0.07	−0.06
Max Temp	−0.519	−0.408	−0.331	−0.06	−0.05	−0.04	−0.546	−0.412	−0.360	−0.06	−0.05	−0.04
Min Temp	0.916	1.751	2.425	0.08	0.16	0.22	1.563	1.716	2.330	0.14	0.15	0.21
Drought	−1.387	−1.097	−0.574	−0.19	−0.15	−0.08	−0.243	−0.065	0.640	−0.03	−0.01	0.09
Wind	−2.902	−1.892	−0.949	−0.14	−0.09	−0.05	−3.200	−3.098	−2.650	−0.16	−0.15	−0.13
Precipitation	−2.622	−1.454	−0.650	−0.10	−0.05	−0.02	−3.772	−2.666	−2.358	−0.14	−0.10	−0.09
Fire	−1.092	−0.879	−0.698	−0.11	−0.09	−0.07	−1.147	−0.320	−0.276	−0.11	−0.03	−0.03
Hail	1.383	2.489	2.883	0.13	0.24	0.27	1.632	2.258	3.286	0.15	0.21	0.31
Panel B												
	$\overline{Q}_2$	A	B	C	D	E	F	G	H	I	J	Median
E3CI/GW	−0.08	−0.07	−0.03	−0.08	−0.13	−0.02	−0.04	−0.25	−0.20	−0.15	−0.08	−0.08
Max Temp/Heat	−0.05	−0.05	−0.03	−0.08								−0.05
Drought	−0.08	−0.01							−0.40			−0.21
Wind/Storms	−0.12	−0.18							−0.03			−0.11
Prec	−0.08	−0.02							−0.18			−0.10
Panel C												
	$\overline{Q}_2$	K	L	M	N	O	Median					
E3CI/GW	−0.43	−0.62	−0.57	−0.23	−0.96	−0.73	−0.62					
Max Temp/Heat	−0.31	−0.09		−0.23		−0.75	−0.23					
Drought	−0.49	−0.34	−0.57			−0.75	−0.57					
Wind/Storms	−0.77	−1.75	−0.40				−1.08					
Prec	−0.57	−0.30	−0.75		−0.96	−0.70	−0.73					

Panel A reports the first (Q1), second (median, Q2), and third (Q3) quartiles of the cross-sectional distribution of impact parameter estimates from the symmetric and asymmetric models for the growth rates of real per capita GDP and GDP. We collect impact parameters by event typology, where the first row, E3CI, refers to the E3CI index impact parameters, and the subsequent rows to each of the E3CI index components: extreme maximum and minimum temperatures, droughts, extreme wind and precipitation, wildfires, and hail. The results reported in the Coefficients columns refer to the actual point estimates, which yield responses to a unitary increase in each indicator. Those reported in the Annual Impact columns refer to the rescaled annual impacts for the growth rates of real per capita GDP and GDP. The normalization yields responses to a typical (1 SD) year-to-year deterioration in extreme weather. Panel B presents the implied average yearly responses of GDP or GDP per capita to a typical worsening in extreme weather conditions. We compute the average of our Q2 estimated GDP and GDP per capita responses to obtain a unified measure of the overall impact on economic growth ($\overline{Q}_2$). We also report results (and their median) from studies A-J described in the text. Panel C reports the implied average yearly responses (and their median) of GDP or GDP per capita to an atypical deterioration in extreme weather conditions, defined as events above the 90th, 95th, or 99th percentile, depending on the study (K-O). In Panels B and C, we also collect impact parameters by event typology, E3CI/GW refers to the E3CI index and global warming in A-O, Max Temp/Heat refers to the extreme maximum temperatures component and heatwave events in A-O; Drought refers to the drought component and drought events in A-O; Wind/Storms refers to the extreme wind component and storm events in A-O; and Prec refers to the extreme precipitation component and rainfall component in A-O.

worked and persons employed), and the real capital stock. On the demand side, we assess the components of GDP expenditure: private consumption, investment, government spending, and net exports.

In Tables 8 and 9 and Figs. 6 and 7, we report selected results for the various demand-side and supply-side variables. Table 8 reports the E3CI results from the symmetric and asymmetric models in (18) and (20). Table 9 reports the results for the various E3CI components from the symmetric models in (19). Detailed results for the asymmetric models in (21) are reported in Tables A7 to A17 in the Online Appendix. Figs. 6 and 7 report the findings of the model averaging analysis using the impact parameters from the symmetric and asymmetric models in (18)–(20) and (19)–(21) for the supply-side and demand-side variables, respectively.

6.1. The supply-side

As shown in Table 8 (first row; columns 1, 2, and 6) and Fig. 6 (first box plot), production efficiency is the primary extreme weather supply-side transmission mechanism. Extreme weather conditions harm all productivity measures. Yet, the effect is more substantial for labor than for total factor productivity. Figures are −8.2%, −2.9%, and −1.4% for GDP per hour worked, GDP per person employed, and total factor productivity, respectively. As shown in Fig. 6 (E3CI boxplots), this finding is robust to specification assumptions, as the impact is negative across all quartiles.

As further shown in Table 8, the adverse effects of extreme weather on productivity are generally more substantial in countries with weaker adaptation and mitigation policies, as well as those with weaker institutions and relatively poorer economic conditions (than more virtuous and affluent countries). For instance, for GDP per person employed, the figures for the less (more) virtuous countries are −5.1% (−1.3%) for adaptation, −3.3% (−2.0%) for mitigation, −4.8% (−2.7%) for institutions' quality, and −3.2% (−0.2%) for income. Consistent with earlier evidence for Europe (e.g., Kotz et al., 2022; Usman et al., 2025; Breckenfelder et al., 2023), we find that climate-induced productivity losses are geographically heterogeneous: the adverse impact is generally more

Table 8
Demand and Supply-side transmission channels, $\widehat{E3CI}$ impact.

	GDP per HW	GDP per EMP	HW	EMP	CAP STOCK	TFP	CONS	INV	GOVT EXP	EXP	IMP	NX
FE	−8.187***	−2.921***	0.350	−0.035	0.201	−1.394*	−1.319*	−4.947*	−0.484	1.847	0.660	1.187
	(1.145)	(0.667)	(0.243)	(0.399)	(0.165)	(0.688)	(0.746)	(2.613)	(1.484)	(1.493)	(2.992)	
Adaptation												
More	−8.685***	−1.253	0.612	−0.621	0.374	−1.166**	−1.460**	−6.451***	−2.294	−0.121	−0.621	0.500
	(1.616)	(0.885)	(0.362)	(0.487)	(0.241)	(0.549)	(0.639)	(2.075)	(1.741)	(1.579)	(2.977)	
Less	−7.697***	−5.045***	−1.029**	0.882	−0.007	−1.898	−0.893	−3.195	1.403	3.942	2.371	1.571
	(2.339)	(1.029)	(0.383)	(0.726)	(0.263)	(1.347)	(1.034)	(3.548)	(1.800)	(2.432)	(3.325)	
Readiness												
More	−8.588***	−1.205	0.420	−0.710*	0.317	−1.231**	−1.781***	−5.848***	−2.252	−0.996	−0.683	−0.313
	(1.713)	(0.757)	(0.361)	(0.411)	(0.215)	(0.515)	(0.625)	(2.112)	(1.551)	(1.487)	(2.930)	
Less	−7.666***	−5.888***	−0.993**	1.308	0.004	−1.921	−0.681	−3.712	1.910	5.684**	2.909	2.775
	(2.395)	(1.224)	(0.423)	(0.825)	(0.307)	(1.613)	(1.122)	(3.730)	(1.912)	(2.500)	(3.480)	
Vulnerability												
Less	−8.290***	−1.526*	0.393	−0.426	0.289	−0.850	−1.206	−5.010*	−1.111	0.788	0.494	0.294
	(1.813)	(0.779)	(0.361)	(0.426)	(0.218)	(0.678)	(0.798)	(2.717)	(1.868)	(1.598)	(3.146)	
More	−8.265***	−5.714***	−0.935**	0.971	0.036	−2.841**	−1.147	−4.568	0.644	3.619	1.093	2.526
	(2.196)	(1.247)	(0.409)	(0.860)	(0.303)	(1.354)	(0.898)	(3.101)	(1.707)	(2.629)	(3.192)	
Mitigation												
More	−9.453***	−1.954**	−0.710	−0.162	0.302	0.844	0.059	−1.153	4.681	1.275	−2.425	3.700
	(2.445)	(0.925)	(0.469)	(0.556)	(0.301)	(0.991)	(1.022)	(5.618)	(2.985)	(2.810)	(4.625)	
Less	−10.663***	−3.273**	−0.283	−0.469	0.349	−0.828	−0.768	−2.660	3.812	−1.634	−2.650	1.016
	(1.961)	(1.369)	(0.586)	(0.734)	(0.505)	(0.936)	(0.952)	(4.174)	(2.601)	(2.886)	(4.167)	
Institutions												
Better	−8.747***	−2.670***	0.358	0.100	0.267	−1.076	−1.404*	−5.020*	−0.840	1.612	0.814	0.798
	(1.064)	(0.691)	(0.242)	(0.387)	(0.181)	(0.662)	(0.796)	(2.720)	(1.506)	(1.561)	(3.046)	
Worse	2.223	−4.830***	−1.393	−1.166	−0.356	−6.728***	−0.594	−4.275	2.415	3.625	−1.003	4.628
	(6.152)	(1.521)	(1.525)	(1.673)	(0.608)	(2.219)	(1.816)	(4.393)	(3.020)	(3.159)	(3.779)	
Income												
Above	−7.722***	−0.221	0.762***	−1.424**	0.150	0.292	−0.033	−9.236***	0.330	3.363	0.919	2.444
	(2.322)	(2.037)	(0.150)	(0.585)	(0.149)	(1.820)	(0.665)	(3.385)	(1.458)	(5.069)	(3.285)	
Below	−8.228***	−3.145***	0.296	0.096	0.207	−1.588**	−1.435*	−4.556*	−0.566	1.704	0.638	1.066
	(1.167)	(0.673)	(0.274)	(0.436)	(0.177)	(0.746)	(0.770)	(2.675)	(1.596)	(1.783)	(3.014)	
Temperature												
Above	−8.419***	−3.423***	0.030	0.204	−0.231	−0.719	−1.271	−3.576	−0.099	4.165	2.782	1.383
	(1.736)	(1.134)	(0.480)	(0.707)	(0.285)	(1.335)	(1.161)	(3.983)	(2.183)	(2.490)	(3.652)	
Below	−8.082***	−2.648***	0.481	−0.153	0.404*	−1.734**	−1.342*	−5.599**	−0.667	0.755	−0.187	0.942
	(1.069)	(0.836)	(0.286)	(0.519)	(0.201)	(0.703)	(0.719)	(2.198)	(1.639)	(1.509)	(2.929)	
Geography												
West	−8.287***	−1.163	0.783***	−0.822**	0.189	−1.019	−1.611*	−5.306*	−1.868	2.454	0.973	1.481
	(1.148)	(0.788)	(0.280)	(0.381)	(0.242)	(0.710)	(0.853)	(2.744)	(1.939)	(1.876)	(3.146)	
East	−7.861***	−5.665***	−0.763*	1.150	0.220	−2.264*	−0.964	−4.508	1.174	1.113	0.211	0.902
	(1.652)	(1.099)	(0.395)	(0.745)	(0.255)	(1.289)	(0.879)	(2.978)	(1.700)	(2.170)	(3.089)	
North	−8.022***	−1.979**	0.616**	−0.514	0.457**	−1.912***	−1.538**	−5.679**	−0.993	−0.911	−0.943	0.032
	(1.005)	(0.777)	(0.285)	(0.476)	(0.208)	(0.650)	(0.613)	(2.288)	(1.601)	(1.315)	(2.920)	
South	−8.576***	−4.494***	−0.320	0.837	−0.270	−0.277	−0.961	−3.738	0.335	6.396**	3.851	2.545
	(1.855)	(1.258)	(0.435)	(0.703)	(0.278)	(1.433)	(1.181)	(3.560)	(2.150)	(2.487)	(3.469)	

This Table reports the E3CI index impact parameter, estimated from the symmetric and asymmetric models, on the growth rates of the supply-side and demand-side variables. Heteroskedasticity-consistent standard errors are in parentheses. Specifically, we report the results from the FE OLS estimation of the symmetric models on the first row (FE). The results reported in the following two rows are for the FE OLS estimation of the asymmetric models, in which the fitted E3CI index is interacted with a dummy variable that controls for the relative level of adaptation (i.e., above or below average). The successive pairs of rows report similar results for the other controls, from the readiness and vulnerability components of the adaptation index through the geographical controls. The supply-side variables are: GDP per hour worked (GDP per HW), GDP per person employed (GDP per EMP), hours worked (HW), persons employed (EMP), the capital stock (CAP STOCK), and total factor productivity (TFP). The demand-side variables are: private consumption (CONS), private investment (INV), government expenditure (GOVT EXP), exports (EXP), imports (IMP), and net exports (NX).

* Denote statistical significance at the 10% level.

** Denote statistical significance at the 5% level.

*** Denote statistical significance at the 1% level.

substantial for Eastern than Western countries (−5.7% vs. −1.2%). Moreover, while labor productivity is most affected in Southern and relatively warmer countries (−4.9% vs. −2.0% for Northern countries), the impact on total factor productivity is largest in Northern and relatively cooler countries (−1.9% vs. −0.3% for Southern countries), echoing the findings of Dellink et al. (2019) and Caggese et al. (2025).

As shown in Table 9, among weather events, extreme precipitation has the most adverse impact on production efficiency. The figures are −5.6%, −5.2%, and −1.1% for GDP per hour worked, GDP per person employed, and total factor productivity,

Fig. 6. Supply-side transmission channels.
Note: The boxplots in this Figure report the results of the model-averaging analysis, using the E3CI index and components' impact parameters estimated from the symmetric and asymmetric models, for the growth rates of the supply-side variables. The E3CI components are extreme maximum and minimum temperatures, droughts, extreme wind and precipitation, wildfires, and hail. The supply-side variables are: GDP per hour worked (GDP per HW), GDP per person employed (GDP per EMP), hours worked (HW), persons employed (EMP), the capital stock (CAP STOCK), and total factor productivity (TFP). Plot (g) shows the averaging of results across all the supply-sided variables in plots (a) to (f) (Supply-side).

respectively. Extreme wind and wildfires follow next. For instance, the figures for GDP per person employed are −3.9% for wind and −1.3% for wildfires. Consistent with Nguyen and Pienknagura (2024), the impact of extreme temperatures on labor productivity is nonlinear, with adverse effects for maximum temperatures (−0.8%) and positive effects for minimum temperatures (+0.9%). The impact of droughts is not clear-cut, while for hail, the effects are positive for all measures and significant for GDP per employed

Table 9
Demand and Supply-side transmission channels, $\widehat{E3CI}$ components impact.

	GDP per HW	GDP per EMP	HW	EMP	CAP STOCK	TFP	CONS	INV	GOVT EXP	EXP	IMP	NX
Max Temp	−1.421***	−0.784***	0.003	0.107	0.114	0.183	−0.658***	−7.662***	0.249	1.445**	1.411*	0.034
	(0.356)	(0.229)	(0.079)	(0.120)	(0.071)	(0.224)	(0.187)	(0.949)	(0.466)	(0.710)	(0.834)	
Min Temp	0.854*	0.846	−0.621**	0.340	−0.302	0.222	4.213**	−8.545	−1.353	−6.924	4.487	−11.411
	(0.464)	(0.629)	(0.280)	(0.371)	(0.203)	(0.484)	(1.952)	(6.918)	(2.522)	(5.948)	(6.121)	
Drought	−0.971*	1.048*	0.212	−1.090**	−0.037	0.150	1.821**	0.206	1.490	−5.258***	1.575	−6.833
	(0.503)	(0.561)	(0.201)	(0.428)	(0.166)	(0.504)	(0.739)	(2.059)	(1.160)	(1.606)	(1.397)	
Wind	−0.681	−3.864***	0.080	0.227	0.578	−0.806	−7.593***	−0.887	−3.716	14.624***	8.907**	5.717
	(1.150)	(1.169)	(0.457)	(0.741)	(0.415)	(1.073)	(1.667)	(6.050)	(2.338)	(4.135)	(4.370)	
Precipitation	−5.625**	−5.167	0.370	1.736*	0.313	−1.142	−4.963***	−0.640	−5.256*	3.256	1.881	1.375
	(2.390)	(1.742)	(0.572)	(0.987)	(0.369)	(1.340)	(1.738)	(5.790)	(2.938)	(4.379)	(4.349)	
Fire	−2.418***	−1.295**	0.178	−0.912***	−0.044	−0.512**	−0.461	−0.019	−2.491***	2.669**	1.650	1.019
	(0.852)	(0.486)	(0.112)	(0.192)	(0.081)	(0.251)	(0.301)	(0.990)	(0.811)	(1.068)	(1.080)	
Hail	0.416	2.050**	0.706**	−0.789	0.256	3.339***	3.645***	5.306	6.396***	0.876	14.023***	−13.147
	(0.734)	(0.765)	(0.282)	(0.550)	(0.162)	(1.205)	(0.749)	(3.274)	(1.578)	(2.553)	(3.094)	

This Table reports the impact of the E3CI index's components on the growth rates of supply-side and demand-side variables, estimated from symmetric models. Heteroskedasticity-consistent standard errors are in parentheses. The E3CI components are extreme maximum and minimum temperatures, droughts, extreme wind and precipitation, wildfires, and hail. The supply-side variables are: GDP per hour worked (GDP per HW), GDP per person employed (GDP per EMP), hours worked (HW), persons employed (EMP), the capital stock (CAP STOCK), and total factor productivity (TFP). The demand-side variables are: private consumption (CONS), private investment (INV), government expenditure (GOVT EXP), exports (EXP), imports (IMP), and net exports (NX).

* Denote statistical significance at the 10% level.

** Denote statistical significance at the 5% level.

*** Denote statistical significance at the 1% level.

person (+2.1%) and total factor productivity (+3.4%). All these findings are also robust to specification choices. As shown in Fig. 6, not only does the median of the effects take negative values for most indicators, but the third quartile does as well. For minimum temperatures, we confirm its positive impact, as the median and third quartile take positive values.

Turning to labor supply, in general, worsening extreme weather conditions increase the number of hours worked and reduce the number of people employed. This pattern holds for Northern and Western European countries and for countries with relatively higher income, which show significant increases in hours worked (+0.8%) and decreases in the number of persons employed (−1.4%). For Eastern European countries and those with lower adaptation scores, the opposite pattern holds, showing a reduction in hours worked and an increase in employment (−1.0% and +1.2%). As shown in Table 9 and Fig. 6, droughts, wildfires, and hail hurt employment (−1.1%), and rising minimum temperatures hurt hours worked (−0.6%). On the other hand, a positive impact of hail on hours worked (+0.7%) and precipitation on employment (1.7%) is notable.

Finally, in general, we find evidence of a positive, albeit non-significant, impact on the rate of capital accumulation (+0.2%). This effect holds for Northern European and cooler countries, as well as for countries with stronger adaptation policies and institutions (+0.3 to +0.5%). This result aligns with the "reconstruction boost" hypothesis, which posits that robust governance and climate readiness facilitate productive recovery investments, as also noted by Bodenstein and Scaramucci (2025). Conversely, countries with weaker institutions, lower adaptation scores, and warmer climates show adverse effects (−0.1% to −0.4%). According to the figures in Table 8, the impact is significant only in relation to the longitude and temperature controls. However, the E3CI box plot reported in Fig. 6 provides full support for the reconstruction effect on capital stock accumulation following extreme weather episodes. Not only the median impact, but also its first quartile, takes positive values for the E3CI index, as well as extreme maximum temperatures, wind, precipitation, and hail. In contrast, we find robust evidence of an adverse effect on capital accumulation rates from rising minimum temperatures and wildfires. Results for drought are not clear-cut.

6.2. The demand-side

Concerning demand-side channels, private spending is the most critical transmission mechanism. As shown in Table 8 (first row, columns 7 through 11), worsening overall extreme weather leads to a significant contraction in both aggregate consumption and investment, i.e., −1.3% and −5.0%, respectively, consistent with precautionary savings, income, and uncertainty effects (see also Usman et al., 2025). As shown in Table 9 and Fig. 7, aggregate consumption is most strongly affected by extreme wind and precipitation, with decreases of −7.6% and −5.0%, respectively. The impact of temperature on consumption is nonlinear, with adverse effects for extreme maximum temperatures (−0.7%) and positive effects for extreme minimum temperatures (+4.0%). The impact of wildfires is negative but not significant (−0.5%). In comparison, droughts and hail may actually trigger an increase in aggregate consumption (+1.8% and +3.7%), potentially consistent with increased government social spending (+1.5% and +6.5%) directed to support affected communities in rebuilding and adaptation activities. We find similar effects on investment for hail (+5.3%) and rising extreme temperatures, both minimum and maximum (−8.6% and −7.7%). The impact of wildfires, extreme wind, and precipitation on investment is negative but not significant (−0.9%). For droughts, the impact is positive but also not significant (+0.2%). The effects on investment growth are broadly consistent with the evidence on capital accumulation.

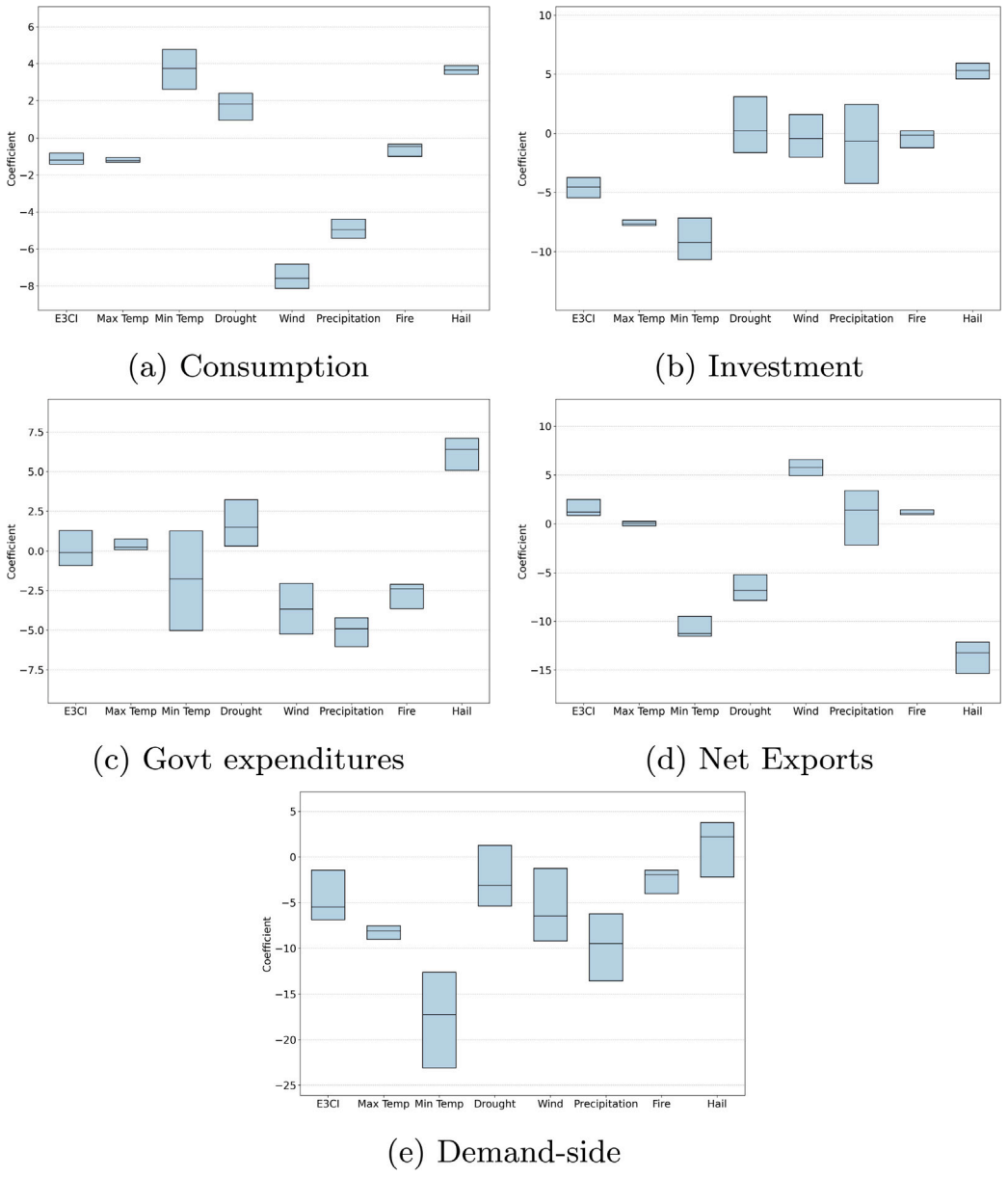

Fig. 7. Demand-side transmission channels.
Note: The boxplots in this Figure report the results of the model-averaging analysis, using the E3CI index and components' impact parameters estimated from the symmetric and asymmetric models, for the growth rates of the demand-side variables. The E3CI components are extreme maximum and minimum temperatures, droughts, extreme wind and precipitation, wildfires, and hail. The demand-side variables are: private consumption (CONS), private investment (INV), government expenditure (GOVT EXP), exports (EXP), imports (IMP), and net exports (NX). Plot (e) shows the averaging of results across all the supply-sided variables in plots (a) to (d) (Demand-side).

As further shown in Table 8 (second row and below, columns 7–11), the adverse impact on consumption and investment is more substantial for Northern, Western, and cooler European countries, and countries with stronger institutions and adaptation policies (−1.6% for consumption; −6.5% for investment). Moreover, the impact on investment is more substantial in relatively higher-income countries than in lower-income countries (−9.2%). In contrast, the effect on consumption is stronger in relatively lower-income countries than in higher-income countries (−1.4%). We also detect a more substantial negative impact on both consumption and investment for countries with weaker mitigation policies (−0.8% and −2.7%).

On the other hand, the effect of deteriorating overall extreme weather conditions is contractionary, yet not significant, for government expenditure (−0.5%). The point estimates of the asymmetric models in Table 8 show an interesting pattern. In general, the response of public spending is contractionary in Northern, Western, and cooler European countries, and in countries with stronger

institutions and adaptation policies, i.e., those whose private spending is mainly affected by climate change (−2.3%). On the other hand, the response of public expenditure is more expansionary for countries with stronger mitigation scores (+4.7%). These effects are imprecisely estimated. As shown in Table 9 and Fig. 7, public expenditure is contractionary in response to extreme wind and precipitation, wildfires, and rising minimum temperature (−1.4% to −5.3%). At the same time, it is expansionary in response to rising maximum temperatures, droughts, and hail (+0.3% to +6.5%). Fig. 7 (panel c) shows that the evidence is robust to specification choices. This mixed evidence, particularly the heterogeneous responses across longitude and latitude, may be partly explained by the presence of public–private mutual insurance schemes in many advanced Northern and Western European countries. These mechanisms are designed to address market failures in insuring highly localized and otherwise uninsurable hazards. By pooling risk and leveraging state support, they provide coverage to the private sector for events that would typically fall outside the scope of conventional insurance. Notable examples include France's CATNAT system, Austria's Catastrophe Fund, and Spain's Consorcio de Compensación de Seguros.

Finally, worsening overall extreme weather conditions appear to exercise an expansionary impact on international trade (Table 8). In fact, the point estimates for exports, imports, and net exports are all positive yet never statistically significant (+1.9%, +0.7%, and +1.2%). The asymmetric responses are also mostly insignificant, yet they exhibit some interesting patterns. For instance, the expansionary impact on net exports is more substantial for Southern, Western, and warmer European countries, as well as for countries with smaller adaptation scores, those that are relatively more affluent, and those with stronger mitigation scores (+1.6% to 4.6%). In terms of event types, as shown in Table 9, expansionary effects are observed for extreme maximum temperatures, wind, precipitation, and wildfires (+1% to +5.7%). On the other hand, contractionary effects are observed for extreme minimum temperatures, droughts, and hail (−6.8% to −13.2%). Overall, our findings are consistent with Dechezlepretre and Sato (2017), who find a limited impact of the EU Emission Trading System (ETS) on firms' competitiveness, possibly due to the generous allocation of free permits. The EU's Carbon Border Adjustment Mechanism (CBAM), expected to be fully operational in 2026, is anticipated to consolidate these results further. As shown in Fig. 7 (panel d), our findings are robust to specification choices.

7. Climate change and structural divergence

Climate change is becoming an increasingly relevant driver of structural economic divergence across Europe, amplifying regional inequalities and challenging cohesion (Breckenfelder et al., 2023). The uneven exposure to climate risks, resulting from climatological and geographical factors, as well as different economic impacts determined by heterogeneous institutions, insurance mechanisms, and investment in mitigation and adaptation, are the primary factors behind this pattern. Bagliano and Morana (2025) show that productivity advancements have been a consistent factor in macro-financial convergence in the Eurozone. In this respect, extreme weather events, through their adverse effects on production efficiency, are likely to consolidate their divergence impact further. The results of the model averaging analysis reported in Fig. 8 provide additional evidence regarding heterogeneous extreme weather effects on an implied broad index of economic activity. The boxplots are, in fact, constructed using the point estimates from the symmetric and asymmetric models for all the variables, including GDP, its sectoral Value-Added decomposition, and supply and demand-side determinants.

Panels *g*, *h*, and *i* in Fig. 8 exhibit evidence on divergence effects through climatological (temperature) and geographical (latitude and longitude) factors. As shown in Panels *g* and *i*, relatively warmer (Southern) and cooler (Northern) countries show a similar negative median response of economic activity to worsening overall extreme weather conditions. Yet, the dispersion of impacts appears larger for warmer than for cooler ones. Extreme precipitation can be singled out as the key driver of the temperature-driven economic divergence, negatively impacting warmer countries to a much greater extent than cooler ones (in terms of both the median level and dispersion). Extreme wind is also a noticeable divergence driver, impacting countries more substantially in cooler regions than in warmer ones. As shown in Panel h, Eastern countries are more severely affected than Western countries, with a larger negative median impact and greater dispersion. Extreme precipitation and wind are the primary sources of latitude-driven economic divergence; rising minimum temperatures and wildfires are also potential contributors, albeit to a lesser extent. By their very nature, climatological and geographical factors are chronic structural drivers of divergence. The Mediterranean region is experiencing more intense and frequent extreme precipitation due to the greater capacity of warmer air to hold moisture, leading to heavier rainfall (Senatore et al., 2025). Winter storms in Northern Europe occur more frequently following strong vortex events than after sudden stratospheric warmings, making cooler regions more exposed to extreme wind events (Afargan-Gerstman et al., 2024). These phenomena are likely to be irreversible and may worsen under unabated climate change.

Panels *a* to *f* in Fig. 8 provide evidence on divergence effects through environmental policy and institutional and economic development factors. In terms of reducing the overall impact of extreme weather, mitigation policies and economic development provide the most effective shields, as the estimated median E3CI impact is negligible in more affluent, environmentally virtuous countries. The same holds, albeit to a lesser extent, for more adapted countries and countries that have implemented better institutions. The results are not surprising, as wealthier countries with stronger institutions tend to benefit from more advanced infrastructure, effective governance, and greater financial resources, which enhance their capacity to fund and implement adaptation and mitigation interventions (Fankhauser and McDermott, 2013). Environmental policies and institutional and economic development appear to be intertwined and mutually reinforcing forces, effective in mitigating the structural divergence impact of climate change. The evidence is clear-cut in relation to extreme precipitations and wind episodes, the two primary sources of climate change-driven economic contractions and structural divergence, conditional on geographical drivers. Mitigation policy and economic development are confirmed to be the most effective corrective actions in this context. On the other hand, albeit to a lesser extent, adaptation policies and institutional development offer a relatively more effective shield against the effects of wildfires and rising extreme temperatures.

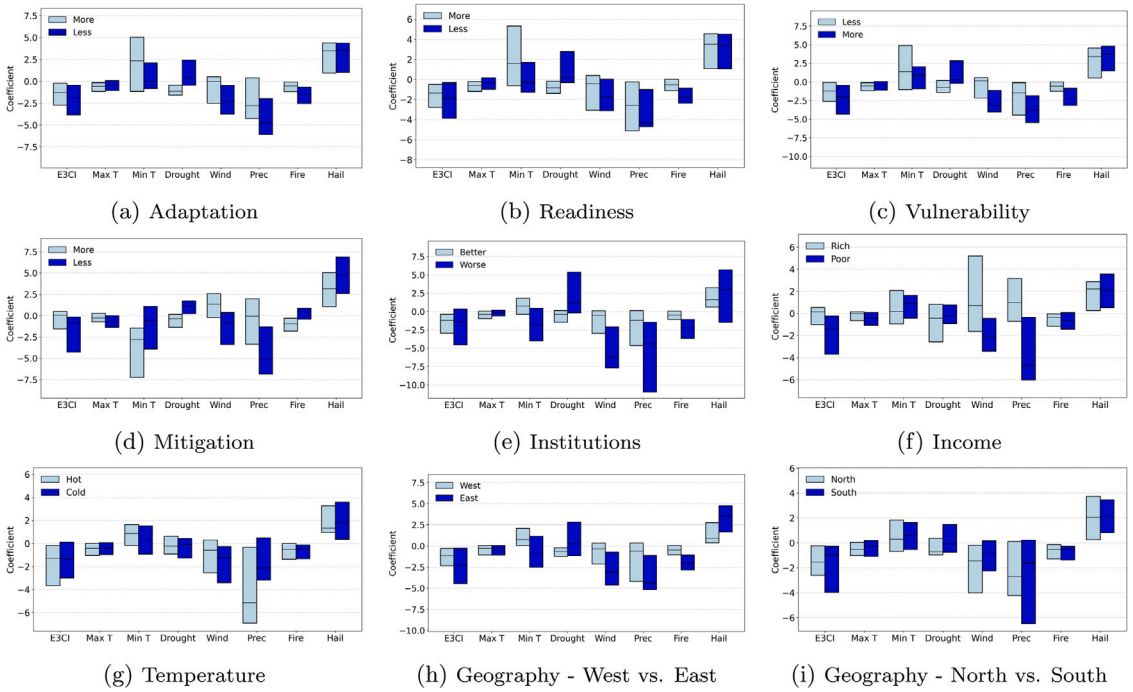

Fig. 8. Adaptation and mitigation policies, institutional and economic development, and climatic zones factors.
Note: The boxplots in this Figure report the results of the model-averaging analysis, using the E3CI index and components' impact parameters estimated from the symmetric and asymmetric models, on the growth rates of an implied measure of real economic activity. The implied measure of real economic activity draws from all the variables assessed in the study: GDP per capita, GDP, Agriculture, Industry, and Service; the supply-side variables, i.e., GDP per HW, GDP per EMP, HW, EMP, CAP STOCK, and TFP; the demand-side variables, i.e., CONS, INV, GOVT EXP, EXP, IMP, and NX. Specifically, the results shown in plot (a) refer to the models in which the fitted E3CI index is interacted with a dummy variable that controls for the relative level of adaptation (i.e., above or below average). The successive plots report similar results for the other controls, from the readiness and vulnerability components of the adaptation index through the geographical controls.

8. Conclusions

In this paper, we offer two main original contributions. First, we investigate the relationship between anthropogenic greenhouse gas (GHG) emissions and underlying extreme weather conditions using a novel panel regression trend-cycle decomposition approach. This methodology might incorporate both human-induced factors – proxied by changes in global atmospheric GHG concentrations – and natural climatic oscillations, allowing for unknown nonlinearities in the linkage between extreme weather and its drivers. It also captures cross-country heterogeneity and commonalities, reflecting the global externality of climate change.

Our analysis draws on the European Extreme Events Climate Index (E3CI) and its seven subcomponents – extreme maximum and minimum temperatures, wind speed, precipitation, droughts, wildfires, and hail – available for 40 European countries since 1981. To our knowledge, this is the first study to exploit this dataset. The results provide robust evidence that extreme weather is statistically and economically linked to both the flow and the stock dimensions of greenhouse gas emissions. While we do not formally establish a causal linkage, exogeneity and asymmetry assumptions, and the robustness of our estimation and modeling strategy, might help bridge the gap to a causal interpretation, supporting the view that anthropogenic GHG accumulation contributes to extreme weather behavior. Moreover, consistent with the global nature of climate dynamics and the influence of long-periodic natural oscillators, we identify a highly nonlinear dominant common component across countries that outweighs idiosyncratic variations.

This finding reinforces the case for coordinated international climate policy, given that Europe is warming at a rate twice the global average and, in a business-as-usual scenario, will continue to do so throughout this century. Without further mitigation policies, land temperatures in Europe are projected to increase by 3.4°C to 8.5°C between 2071 and 2100, according to scenarios (EEA, 2024a,b,c). Establishing a clear connection between the climate-warming effects of GHGs and worsening extreme weather conditions is instrumental in shaping evidence-based policy interventions to mitigate the impact of human activity on the natural environment. While most of the previous contributions in the climate econometrics literature have dealt with the linkages between GHG emissions and global warming (Kaufmann et al., 2006, 2013; Estrada et al., 2013a,b; Estrada and Perron, 2017; Morana and Sbrana, 2019), this paper goes further and assesses linkages between evolving extreme weather conditions and GHG emissions.

Second, climate change is not only an environmental issue but also a macroeconomic disruptor and a source of structural divergence for the European economy. We then exploit the above findings and assess the economic impact of the multifaceted dimensions of underlying deteriorating weather conditions on GDP growth and the sectoral composition of gross Value-Added, as

well as its demand- and supply-side transmission mechanisms. We focus on production efficiency, labor supply, capital accumulation on the supply side, and components of GDP expenditure on the demand side. In our analysis, we explicitly control for heterogeneities arising from varying attitudes toward environmental policy, institutional quality, income levels, and geographical factors. We conduct the empirical analysis using dynamic panel regressions within an Autometrics (Hendry et al., 2008) framework and model averaging. By conditioning on the extreme-weather trend components driven by radiative forcing, we avoid potential downward bias arising from unrelated short-periodic natural phenomena and observational noise. We complement existing studies by offering broader geographic coverage (beyond the EU), a more comprehensive treatment of extreme weather typologies, and an in-depth analysis of demand- and supply-side transmission mechanisms, using new econometric tools.

We find that deteriorating extreme weather conditions lead to a significant contraction in European GDP growth, with all major sectors experiencing losses. The impact is strongest in services, followed by industry, and smallest, though still negative, in agriculture. Among the various hazards, extreme wind and precipitation events generate the largest economic damage. Overall, our estimates point to a median annual GDP decline of −0.08% under a business-as-usual scenario, cumulating to roughly −2.2% by 2050 and −6.2% by 2100. Our predictions are consistent with the median predicted GDP costs of typical extreme weather developments in the literature. These figures should be viewed as conservative, as they do not account for atypical or tail-risk manifestations of extreme weather, which are associated with substantially larger economic impacts.

Deteriorating extreme weather conditions impact GDP growth through both demand- and supply-side channels, with private spending and productivity as the most critical. We also detect mechanisms through which climate change is contributing to structural economic divergence in Europe. Labor productivity is primarily affected in Southern European and relatively warmer countries, while total factor productivity is affected mainly in Northern European and relatively cooler countries. Efficiency losses are also more substantial for Eastern countries than for Western ones. They are also, in general, larger in countries with weaker adaptation and mitigation policies, as well as those with weaker institutions and relatively less affluent economies. The impact on aggregate consumption and investment is also more substantial for countries with weaker mitigation policies. Yet, the adverse effect on private spending responses appears to be more significant for Northern, Western, and cooler European countries, as well as for countries with stronger institutions and adaptation policies.

In terms of policy implications, mitigation policy and (sustainable) economic development appear to be the most effective ways to lessen the contribution of deteriorating extreme weather conditions to economic stagnation and structural divergence, particularly from extreme precipitation and wind. Adaptation policy and institutional development are only a second best in this respect, offering a relatively more effective shield against wildfires and rising extreme temperatures. Hence, despite the chronic nature of climate change's economic impact, policy instruments to mitigate its recessionary and structural divergence effects are available. In this respect, integrating climate resilience into the EU cohesion policy has been an essential first step toward developing a robust framework to fund climate change mitigation and adaptation, promote sustainable development across all European regions, and avoid the deepening of regional disparities. As Europe faces unprecedented external challenges since the end of the Cold War, integrating energy security and climate policy appears to be the next necessary step. Mario Draghi's 2024 report on European competitiveness has paved the way for the European Green Deal to become the European strategy for sovereignty, resilience, and competitiveness (Draghi, 2024; EC, 2025). This transformation is necessary to avoid a trade-off between the Green Deal and increased defense spending. To meet EU climate targets, public investment must increase by 2% of GDP annually, or approximately €300–350 billion per year. In comparison, defense spending is projected to rise from 2% to 3.5% of GDP, requiring an additional €250 billion per year. While the European Commission's emergency clause allows for temporary deviations from fiscal rules to boost defense spending, a reform of the Stability and Growth Pact to eliminate hindrances to member countries' productive public investment appears as necessary as ever.

Declaration of competing interest

The authors declare that they have no known competing financial interests or personal relationships that could have appeared to influence the work reported in this paper.

Appendix A. Supplementary data

Supplementary material related to this article can be found online at https://doi.org/10.1016/j.euroecorev.2026.105327.

Data availability

Data will be made available on request.

References

Afargan-Gerstman, H., Büeler, D., Ole Wulff, C., Sprenger, M., Domeisen, D.I.V., 2024. Stratospheric influence on the winter North Atlantic storm track in subseasonal reforecasts. Weather. Clim. Dyn. 5, 231–249.

Ascoli, D., Moris, J.V., Marchetti, M., Sallustio, L., 2021. Land use change towards forests and wooded land correlates with large and frequent wildfires in Italy. Ann. Silvic. Res. 46, 177–188.

Auffhammer, M., 2018. Quantifying economic damages from climate change. J. Econ. Perspect. 32, 33–52.

Bagliano, F.C., Morana, C., 2025. Eurozone economic integration: Historical developments and new challenges ahead. Eur. Econ. Rev. 176.

Baiardi, D., Morana, C., 2021. Climate change awareness: Empirical evidence for the European Union. Energy Econ. 96, 1–16.

Becker, R., Enders, W., Lee, J., 2006. A stationarity test in the presence of an unknown number of smooth breaks. J. Time Series Anal. 27, 381–409.

Bier, V.M., 2017. Understanding and mitigating the impacts of massive relocations due to disasters. Econ. Disasters Clim. Chang. 1, 179–202.

Bijnens, G., Anyfantaki, S., Colciago, A., De Mulder, J., Falck, E., Labhard, V., Lopez-Garcia, P., Meriküll, J., Parker, M., Röhe, O., Schroth, J.a., 2024. The Impact of Climate Change and Policies on Productivity. Occasional Paper Series 340, European Central Bank.

Bilal, A., Kanzig, D.R., 2024. The Macroeconomic Impact of Climate Change: Global Vs. Local Temperature. National Bureau of Economic Research Working Paper, no. 32450.

Bilal, A., Stock, J.H., 2025. Macroeconomics and Climate Change. NBER Working Paper No. 33567, March 2025.

Bodenstein, M., Scaramucci, M., 2025. On the GDP effects of severe physical hazards. Eur. Econ. Rev. 175.

Breckenfelder, J., Mackowiak, B., Marques, D., Olovsson, C., Popov, A., Porcellacchia, D., Schepens, G., 2023. The Climate and the Economy. ECB Discussion Paper Series no. 22.

Breitung, J., Kripfganz, S., Hayakawa, K., 2022. Bias-corrected method of moments estimators for dynamic panel data models. Econ. Stat. 24, 116–132.

Burke, M., Hsiang, S.M., Miguel, E., 2015. Global non-linear effect of temperature on economic production. Nature 257, 235–239.

Caggese, A., Chiavari, A., Goraya, S.S., Villegas-Sanchez, C., 2025. Climate Change, Firms, and Aggregate Productivity. ECB Working Paper no. 3084.

Canepa, A., 2025. Two Decades on: Assessing the Impact of the Copenhagen Criteria on Environmental Performance in the 2004 EU Accession Countries. ESt Working Paper Series 01/25.

Casey, G., Fried, S., Goode, E., 2023. Projecting the impact of rising temperatures: The role of macroeconomic dynamics. IMF Econ. Rev. 71, 688–718.

Cassola, N., Morana, C., Ossola, E., 2025. Climate change risk pricing in the European stock market. Appl. Econ. 57, 10081–10103.

Cortés Arbués, I., Chatzivasileiadis, T., Ivanova, O., Storm, S., Bosello, F., Filatova, T., 2024. Distribution of economic damages due to climate-driven sea-level rise across European regions and sectors. Sci. Rep. 14, 126.

Dechezlepretre, A., Sato, M., 2017. The impacts of environmental regulations on competitiveness. Rev. Environ. Econ. Policy 11, 183–206.

Dellink, R., Lanzi, E., Chateau, J., 2019. The sectoral and regional economic consequences of climate change to 2060. Environ. Resour. Econ. 72, 309–363.

Devot, A., Royer, L., Arvis, B., Deryng, D., Giauffret, E.Caron., Giraud, L., Ayral, V., Rouillard, J., 2023. Research for AGRI Committee – the Impact of Extreme Climate Events on Agriculture Production in the EU. European Parliament, Policy Department for Structural and Cohesion Policies, Brussels.

Dietz, S., Lanz, B., 2025. Growth and adaptation to climate change in the long run. Eur. Econ. Rev. 173, http://dx.doi.org/10.1016/j.euroecorev.2025.104982, forthcoming.

Draghi, M., 2024. The future of European competitiveness. Avaialble at https://commission.europa.eu/topics/eu-competitiveness/draghi-report_en%#paragraph_47059.

EC, 2025. The Draghi report: One year on. Avaialble at https://commission.europa.eu/topics/eu-competitiveness/draghi-report/one-year-after_en.

EEA, 2024a. Global and European temperatures. Available at https://www.eea.europa.eu/en/analysis/indicators/global-and-european-temperatures.

EEA, 2024b. Economic losses from weather- and climate-related extremes in Europe. Available at https://www.eea.europa.eu/en/analysis/indicators/economic-losses-from-climate-related.

EEA, 2024c. Europe's warmest year on record—Striking climate contrasts in 2024. Available at https://www.copernicus.eu/en/news/news/observer-europes-warmest-year-record-striking-climate-contrasts-2024.

Estrada, F., Perron, P., 2017. Extracting and analyzing the warming trend in global and hemispheric temperatures. J. Time Series Anal. 38, 711–732.

Estrada, F., Perron, P., Gay-Garcia, C., Martinez-Lopez, B., 2013a. A time-series analysis of the 20th century climate simulations produced for the IPCCs Fourth Assessment Report. PLoS One 1–10.

Estrada, F., Perron, P., Martinez-Lopez, B., 2013b. Statistically derived contributions of diverse human influences to twentieth-century temperature changes. Nat. Geosci. 6, 1050–1055.

ESWD, 2023. European severe weather database. Available at https://eswd.eu/cgi-bin/eswd.cgi.

Fankhauser, S., McDermott, T.K.J., 2013. Understanding the Adaptation Deficit.Why are Poor Countries more Vulnerable To Climate Events than Rich Countries?. Grantham Research Institute on Climate Change and the Environment WP no. 134.

Felbermayr, G., Gröschl, J., 2014. Naturally negative: The growth effects of natural disasters. J. Dev. Econ. 111, 92–106.

Gagliardi, N., Arévalo, P., Pamies, S., 2022. The Fiscal Impact of Extreme Weather and Climate Events: Evidence for EU Countries. European Commission Discussion Paper no. 168.

García-León, D., Casanueva, A., Standardi, G., Burgstall, A., Flouris, A.D., Nybo, L., 2021. Current and projected regional economic impacts of heatwaves in Europe. Nat. Commun. 12, 5807, 1-10.

Guo, J., Kubli, D., Saner, P., 2021. The Economics of Climate Change: Noaction Not an Option. Swiss Re, Zurich.

Hausman, J., Pinkovskiy, M.L., 2017. Estimating Dynamic Panel Models: Backing Out the Nickell Bias. CeMMAP working papers 53/17, Institute for Fiscal Studies.

Hendry, D.F., Johansen, S., Santos, C., 2008. Automatic selection of indicators in a fully saturated regression. Comput. Statist. 33, 317–335.

Hsiao, C., Zhang, J., 2015. IV, GMM or likelihood approach to estimate dynamic panel models when either N or T or both are large. J. Econometrics 187, 312–322.

Kahn, M.E., Mohaddes, K., Ng, R.N., Pesaran, M.H., Raissi, M., Yang, J.-C., 2021. Long-term macroeconomic effects of climate change: A cross-country analysis. Energy Econ. 104, 105–124.

Kaufmann, R.K., Kauppi, H., Mann, M.L., Stock, J.H., 2013. Does temperature contains a stochastic trend: linking statistical results to physical mechanisms. Clim. Change 118, 729–743.

Kaufmann, R.K., Kauppi, H., Stock, J.H., 2006. The relationship between radiative forcing and temperature: what do statistical analyses of instrumental temperature record measure? Clim. Change 77, 279–289.

Kiley, M.T., 2024. Growth at risk from climate change. Econ. Inq. 62, 1134–1151.

Kimmich, C., Weyerstraß, K., Czypionka, T., Fauster, N.F.R., Kinner, M., Laa, E., Mateeva, L., Plank, K., Ulrici, L., Zenz, H., Miess, M., Poledna, S., 2025. Economic impact of labor productivity losses induced by heatstress: An agent-based macroeconomic approach. Clim. Change 178 (3), 36.

Kotz, M., Levermann, A., Wenz, L., 2022. The effect of rainfall changes on economic production. Nature 601, 223–227.

Morana, C., 2024. A new macro-financial condition index for the euro area. Econ. Stat. 29, 64–87.

Morana, C., Sbrana, G., 2019. Climate change implications for the catastrophe bonds market: An empirical analysis. Econ. Model. 81, 274–294.

Muller, U., Watson, M., 2018. Long-Run covariability. Econometrica 86, 775–804.

Natoli, F., 2023. The Macroeconomic Effects of Temperature Surprise Shocks. Bank of Italy Temi di Discussione (Working Paper), no. 1407.

Nguyen, H., Pienknagura, S., 2024. Rising Temperature, Nuanced Effects: Evidence from Seasonal and Sectoral Data. IMF Working Paper No. 2024/202.
Noy, I., Strobl, E., 2023. Creatively destructive hurricanes: Do disasters spark innovation? Environ. Resour. Econ. 84, 1–17.
Orlov, A., Sillmann, J., Aunan, K., Kjellstrom, T., Aaheim, A., 2020. Economic costs of heat-induced reductions in worker productivity due to global warming. Glob. Environ. Chang. 63, 102087.
Parker, M., 2023. How climate change affects potential output. Eur. Cent. Bank Econ. Bull. (6/2023), URL: https://www.ecb.europa.eu/press/economic-bulletin/articles/2023/html/ecb.ebart202306_02%~0535282388.en.html.
Philippon, T., 2022. Additive Growth. National Bureau for Economic Research Working Papers Series, no. 29950.
Robinson, W.A., 2021. Climate change and extreme weather: A review focusing on the continental United States. J. Air Waste Manage. Assoc. 71, 1186–1209.
Senatore, A., Furnari, L., Nikravesh, G., Castagna, J., Mendicino, G., 2025. Increasing daily extreme and declining annual precipitation in Southern Europe: A modeling study on the effects of Mediterranean warming. EGUsphere http://dx.doi.org/10.5194/egusphere-2025-1567, forthcoming.
Stock, J.H., 1988. Estimating continuous-time processes subject to time deformation, An application to postwar U.S. GNP. Joumal Amer. Stat. Assoc. 83, 77–85.
Swanson, K.L., Sugihara, G., Tsonis, A., 2009. Long-term natural variability and the 20th century climate change. Proc. Natl. Acad. Sci. (PNAS) 106, 16120–16123.
Szewczyk, W., Feyen, L., Matei, A., Mulholland, E., Soria, A., 2020. Economic Analysis of Selected Climate Impacts. EUR 30199 EN, Publications Office of the European Union, Luxembourg, ISBN: 978-92-76-18459-1, http://dx.doi.org/10.2760/845605,JRC120452.
Usman, S., Fernandez, G.G.T., Parker, M., 2025. Going NUTS: the regional impact of extreme climate events over the medium term. Eur. Econ. Rev. 178.
Wu, Z., Huang, N.E., Wallace, J.M., Smoliak, B.V., Chen, X., 2011. On the time varying trend in global mean surface temperature. Clim. Dyn. 37, 759–773.
Xu, G., et al., 2024. Jet stream controls on European climate and agriculture since 1300 ce. Nature 634, 600–608.